Aus dem Institut für Physiologie der Universität Tübingen

Abteilung für Neurophysiologie

Dopaminergic neurons and microglia shift in mice induced-by CCl4

Inaugural-Dissertation
zur Erlangung des Doktorgrades
der Medizin

der Medizinischen Fakultät
der Eberhard Karls Universität
zu Tübingen

vorgelegt von

Wang, Hui

2022

Dekan:	Professor Dr. B. Pichler
1. Berichterstatter	Professorin Dr. O. Garaschuk
2. Berichterstatter:	Professor Dr. P. Kahle

Tag der Disputation: 28.01.2022

Table of Contents

List of figures

List of tables

List of abbreviations

AD	Alzheimer’s disease
AHD	acquired hepatocerebral degeneration
AST	aspartate aminotransferase
BBB	blood-brain barrier
BMECs	brain microvascular endothelial cells
CCl4	carbon tetrachloride
CNS	central nervous system
CVOs	circumventricular organs
DAT	dopamine transporter
D2R	dopamine 2 receptor
HE	hepatic encephalopathy
i.p.	intraperitoneally
IL-1	interleukin- 1
IL-6	interleukin- 6
LPS	lipopolysaccharide
MCP-1	monocyte chemoattractant protein-1
MPP^+	1-methyl-4-phenylpyridium
MIP	Maximum-intensity projection
NeuN	neuronal nuclei
NF-κB	nuclear transcription factor-kappa B
OFT	open field test
PD	Parkinson’s disease
PMT	photomultiplier tubes

SNc	substantia nigra compacta
SNr	substantia nigra reticulata
SPECT	single-photon emission computed tomography
TH	tyrosine hydroxylase
TNF- α	tumour necrosis factor-alpha
VTA	ventral tegmental area

1. Introduction

Liver-brain axis in liver failure

There is growing evidence showing that the range of complications in chronic liver diseases are not limited to the liver, but comprise several organs, especially the brain. Liver inflammation and fibrosis are the cardinal pathological progression of almost all liver diseases. In this section, the preliminary work on the Liver-brain axis with special emphasis on inflammation and fibrosis is described.

1.1. Inflammation

Inflammatory triggers, such as viruses, bacteria, and toxins can activate Kupffer cells, specialized macrophages of the liver, thereby leading to the emergence of liver inflammation. It has been suggested that inflammation, induced by liver diseases, can affect the central nervous system (CNS) (Garcia-Martinez and Cordo Ba 2012) by increasing the systemic levels of pro-inflammatory cytokines (e.g., TNF-α, IL-1ß, IL-6) (Butterworth and Roger 2013a). Indeed, high serum levels of pro-inflammatory cytokines, including TNF-α, IL-1ß, IL-6, were detected in patients with different chronic liver diseases (Tilg 1992). Furthermore, after systemic administration of lipopolysaccharide (LPS), a classic drug that increases the level of peripheral inflammatory cytokines, rodents show behavioural impairments consistent with the involvement of the CNS, although the underlying mechanisms are not entirely clear (D'Mello and Swain 2016). Even though the CNS is persistently sheltered by the blood-brain barrier (BBB), several potential signalling pathways exist, which might be relevant for the liver-brain inflammation axis, namely the neural, humoral, and immune pathways (D'Mello and Swain 2011).

Neural pathway: Vagal afferents are considered as a potential pathway for the communication between the liver and the brain, as well as between the gut and the brain. The vagal nerve, which expresses cytokine receptors, can be activated when exposed to cytokines. Thereby, the afferent vagus nerve through the nucleus tractus solitarius

transmits signals to multiple brain regions and nuclei, including the parabrachial and hypothalamic paraventricular nuclei, ultimately leading to cognitive and behavioural changes (Goehler et al. 2000). Interestingly, neurological dysfunction in the patient with primary biliary cirrhosis did not benefit from liver transplantation (D'Mello et al. 2011, Mcdonald et al. 2010). This suggested that the neural pathway is not the sole link in the liver-brain axis.

Humoral pathway: Brain microvascular endothelial cells (BMECs), a major component of the BBB, express multiple cytokine receptors, which comprise TNFR1 and TNFR2, as well as IL-1R1 and IL-6R. Activation of these receptors by serum cytokines is another pathway connecting the periphery with the CNS. During sustained exposure to the pro-inflammatory cytokines, BMECs were observed to generate prostaglandins and nitric oxide, which can be released into the brain parenchyma and thereby induce neuroinflammation (D'Mello et al. 2011). Furthermore, the circumventricular organs (CVOs), a region with BBB deficiency, allow peripheral inflammatory molecules to directly enter the CNS.

Immune pathway: Microglia, the main immune cells of the brain, which are constantly monitoring the brain microenvironment, can also be activated by peripheral inflammation (Henry et al. 2009, Qin et al. 2010). On the one hand, activated microglia express the monocyte chemoattractant protein-1 (MCP-1) promoting the recruitment of monocytes into the brain. On the other hand, the monocytes can infiltrate into the brain directly. It is well known that both activated microglia and infiltrating monocytes corporately produce inflammatory cytokines, which cause changes in neurotransmission and behaviour. For instance, the peripheral administration of TNF-α results in increased TNF-α and IL-1β levels within the rodent brain (Qin et al. 2010). Besides, the microglia activation and increased proinflammatory cytokines (TNF-α, IL-1, IL-6) were observed in the brain of rodents peripherally administered with LPS (Henry et al. 2008, Ransohoff and Perry 2009).

1.2. Chronic liver fibrosis

The liver plays a vital role in breaking down toxins and purifying the blood, thereby, protecting the multiple organs from hazardous substances (Santoro et al. 2007). Neurological complications are common in patients with chronic liver diseases, including hepatic encephalopathy (HE), acquired hepatocerebral degeneration (AHD) and other neuropsychiatric symptoms (Sureka et al. 2015). These neurological disorders seem to be attributed to the following: the vast accumulation of toxins (e.g., ammonia, lactate, manganese) in the brain; the subsequent activation of microglia; the dysfunction in astrocytes and neurons; the occurrence of neuroinflammation; the increased BBB permeability (Butterworth 2011). The CNS deficits caused by liver diseases are diverse, and the causes are complicated. Here, we focus on cirrhosis-related Parkinsonism.

Clinically, the symptoms of cirrhosis-related Parkinsonism were characterized as a bilateral akinetic-rigid syndrome, lacking resting tremor (Burkhard et al. 2003). Liver fibrosis can cause attenuated detoxification and portosystemic venous shunting further leading to the accumulation of elevated ammonia or manganese in the brain. Indeed, the deposition of manganese in the basal ganglia has been demonstrated in over 80% of cirrhotic patients utilizing neuroimaging techniques, and in patients with cirrhosis, the incidence of Parkinsonism was estimated to be 21% (Butterworth and Roger 2013b). Moreover, the epidemic study has shown that workers in high-manganese (Mn) environments are more likely to develop Parkinsonism (Levy et al. 2003). Is cirrhosis-related Parkinsonism simply caused by excessive Mn poisoning?

Indeed, the role of Mn for the pathogenesis of cirrhosis-related Parkinsonism has been recognized and it was shown that excessive Mn primarily causes degeneration of globus pallidus, in contrast to classic Parkinson's disease (PD), which is mainly caused by the dopaminergic neuronal damage in the midbrain (Butterworth et al. 2013b, Perl and Warren 2007). An additional possible hypothesis is a disturbance of the dopaminergic neurotransmission due to the accumulation of toxins including ammonia, Mn, and inflammatory triggers (Butterworth et al. 1996).

Under physiological conditions, the dopamine released from the presynapse can bind to the postsynaptic D1 or D2 receptors (D1R or D2R) to activate the dopaminergic signalling cascade and the remaining dopamine is recycled by the presynaptic dopamine transporter (DAT). Weissenborn and colleagues, through the detection of single-photon emission computed tomography (SPECT) technology, found a selective loss of presynaptic DAT sites and postsynaptic D2R sites in patients with cirrhosis and presenting with Parkinsonism (Weissenborn et al. 2000). Kim et.al analyzed 5 patients with cirrhosis merged with Parkinsonism to assess DAT density. They concluded that four of five patients differed from idiopathic PD, as normal DAT density, non-progressive symptoms, and ineffectiveness of levodopa treatment were found in liver cirrhosis-related Parkinsonism (Kim et al. 2010).

Interestingly, Shinotoh et.al measured the synaptic dopaminergic function in four patients with chronic Mn intoxication, they found that synapses and nigrostriatal dopaminergic function are almost normal in these patients, which means that the aetiology of Parkinsonism caused by chronic Mn intoxication is different from that of cirrhosis-related Parkinsonism (Shinotoh et al. 1997). Taken together, these data suggest that both degeneration of globus pallidus, induced by excessive Mn, and disturbance in the dopaminergic neurotransmitter system, contributed by other factors (e.g., ammonia or neuroinflammation), might synergistically lead to cirrhosis-related Parkinsonism (Butterworth et al. 2013b).

It is well established that liver inflammation and fibrosis can be induced by carbon tetrachloride (CCl4) (Rocha et al. 2014, Sha et al. 2020, Tan et al. 2016). CCl4 is metabolized by the hepatocytes to form the toxic trichloromethyl radical (CCl•3), which can disrupt lipid metabolism, and reduce the amount of protein in the normal cell. Further, the CCl•3 can trigger genetic mutations inducing liver cancer. In addition, the trichloromethylperoxy radical (CCl3OO•), generated by the oxidation of CCl•3, further triggers lipid peroxidation and destroys polyunsaturated fatty acids. Thus, the plasma membrane becomes more permeable, consequently disrupting homeostasis and leading

to hepatic inflammation, fibrosis, cirrhosis, and cancer (Liedtke et al. 2013, Paquet and Kamphausen 1975, Scholten et al. 2015).

In summary, although the connection between cirrhosis and Parkinsonism seems to be well established, the underlying cellular/molecular mechanisms are not completely understood. Although inflammatory processes, as well as accumulation of toxic substances (ammonia, manganese), might play a role, the pathological changes and underlying mechanisms in cirrhosis-related Parkinsonism need further exploration.

Parkinsonism in liver failure

1.3. Neurons

PD is the second most common neurodegenerative disease, after Alzheimer's disease (AD). The clinical manifestation mainly involves bradykinesia, rigidity, static tremor, festinating gait, and other non-motor symptoms (Mhyre et al. 2012, Shulman et al. 2002). The post-mortem pathology comprises a massive loss of dopaminergic neurons in the substantia nigra compacta (SNc) and aggregation of novel protein (α-synuclein) in the brain of PD patients (Surmeier et al. 2017). Generally, the dopaminergic pathway can be divided into 4 major embranchments: the nigrostriatal, tuberoinfundibular, mesolimbic and mesocortical system (Cousins et al. 2010).

The dopaminergic neurons are mainly distributed in the SNc and ventral tegmental area (VTA) of the midbrain. Whereas the dopaminergic neurons in the SNc primarily project to the dorsal striatum, contributing to the formation of the nigrostriatal system, the dopaminergic neurons in the VTA mainly project to the ventral striatum and the prefrontal cortex, thus establishing the mesolimbic and mesocortical pathways respectively (Meck 2006). Nevertheless, the damage of VTA during the progress of PD is negligible. By contrast, the loss of dopaminergic neurons in the SNc and the subsequent dopamine deficiency in the basal ganglia region is considered as the main cause of the motor symptoms in PD (Eriksen et al. 2009). Thus, the mainstay of therapy in relieving the motor symptoms is a medication with levodopa leading to higher levels of dopamine, or drugs that stimulated dopamine receptors directly.

Clinically, the widespread distribution of α-synuclein in the brain, not just in the substantia nigra (SN), is thought to be responsible for the psychological impairment in patients with PD (Surmeier et al. 2017). Also in chronic liver disease, which can lead to multiple neurodegenerative diseases, such as AHD, post-shunt myelopathy, and cerebella degeneration, there is considerable evidence for neuronal loss (Butterworth et al. 2013b). Moreover, neuronal loss in cirrhosis occurs in several areas of the brain, including the basal ganglia, cerebellum, thalamus, pons, spinal cord, and cerebral cortex (Butterworth et al. 2013b). However, to date, there is no definite evidence demonstrating in patients with hepatic Parkinsonism neuronal loss in the SN. Instead, a growing body of evidence suggests that this type of Parkinsonism was mostly attributed to the loss of presynaptic DAT sites and postsynaptic D2R sites in the basal ganglia. Nevertheless, the dopaminergic neuron lesions were observed at the end stage of hepatic cirrhosis, owing to the accumulation of excessive neurotoxins, production of inflammatory cytokines, and free radicals (Victoria et al. 2017).

1.4. Microglia

Microglia under physiological conditions have a highly ramified morphology and play a critical role in immune surveillance (Morris et al. 2013, Perry et al. 2010b, Toguchi et al. 2009). The stimuli derived from injury, inflammation, neurotoxins, or aberrant protein accumulation, can lead to microglial activation and alteration of microglial morphology. Once the microglia activation is initiated, the cells increased soma size and shorten their processes, in an extreme case transforming into phagocytic amoeboid microglia (Ling and Wong 2010). The activated microglia can up regulate the expression of macrophage/myeloid-associated antigen (CD 68) in the lysosomal membranes. The latter is a marker of the phagocytic function of activated microglia. On the other hand, proliferation and migration of microglia were also observed during neuroinflammation (Perry and Teeling 2013).

Recent evidence suggests that neuroinflammation can be triggered by peripheral inflammation, and thereby might contribute to the neurotoxic effect in the nigrostriatal

pathway, which is characterized by microglial activation (Subramaniam and Federoff 2017). It has previously been observed that the classic inflammatory stimuli (e.g., LPS), can cause rapid and significant microglial activation and the loss of dopaminergic neurons in SNc in rodents (Claudia et al. 2014, Gayle et al. 2002, Tanaka et al. 2013). The old view is that microglia can adopt one of the two distinctive phenotypes, pro-inflammatory M1 or anti-inflammatory M2 phenotypes. The majority of studies on microglial phenotypes suggests the dominance of M1 microglia in patients with AD and PD (Tang and Le 2016). Most studies, however, have failed to precisely address the time course and relationship between microglia activation and neuronal loss under these conditions. Interestingly, the study found that the process of neuronal loss was initiated by the occurrence of pro-inflammatory microglia, and the cessation of neuronal loss was likely due to the shift in microglial phenotype from M1 to M2 (Beier et al. 2017). However, in this study, the microglia have only been analyzed in the striatum, but not in SN. Moreover, nowadays it is accepted that microglia activation rather takes place in a continuum, and cannot be simply classified as M1 or M2. Therefore, the dynamic changes in microglia require more detailed observation and detection.

Together, it is well established that loss of dopaminergic neurons occurs under conditions of strong systemic inflammation or in models of liver cirrhosis. However, the time course of neuronal loss and the relation between the loss of neurons and activation of microglia remains to be determined.

1.5. Aims of this research project

1.) To study whether dopaminergic neurons and microglia in SN are more vulnerable than that of VTA in C57BL/6J mice treated with CCl4.

2.) To study whether the extent of neuronal loss was aggravated in the mice of severe fibrosis, compared with the mice of mild fibrosis.

3.) To reveal the temporal and spatial relationship between the loss of dopaminergic neurons and the activation of microglia in SN of mice treated with CCl4.

4.) To study whether the liver inflammation induced by CCl4 can cause parkinsonian symptoms.

2. Material and methods

2.1. Animal treatment

All animal experiments were conducted by our collaborators at the Hannover Medical University, license number 33.12-42502-04-20/3392. The isolated tissues were stained with respective antibodies, imaged and analyzed in Tübingen. Analyses of the animal behaviour were also conducted in Tübingen. C57BL/6J mice aged 5-9 weeks were used in our study, the animals were divided into three groups (n = 4–10 mice per group): (1) "Control" with the administration of 0.9% NaCl; (2) "Vehicle" with the administration of sunflower oil; (3) "CCl4" with the administration of CCl4 dissolved in sunflower oil (0.4 µl/g). It is well established that 2-4 weeks of CCl4 administration via intraperitoneal injections in mice can cause mild fibrosis, severe liver fibrosis can be detected after 6-8 weeks of treatment (Scholten et al. 2015). Here, intraperitoneal injections were administered either once or twice a week for (i) 4 and (ii) 9 weeks. The mice were sacrificed either 36 hours after a single injection or after 4 or 9 weeks of treatment. Brain, blood and liver samples were collected for further experiments.

2.2. Immunofluorescence

The brain tissues were fixed overnight at 4℃ with 4% formaldehyde, then transferred in PBS with 25% sucrose overnight at 4℃. Afterwards, embedded and

stored in the refrigerator at -80 ℃.

Coronal slices (thickness 50μm) were cut, then sections were twice rinsed for 10 min in PBS. To avoid non-specific background staining, the slices were treated with 200 μl blocking solution (5% normal donkey serum and 1% Triton-X 100 in PBS) for 1 h. Then, the primary antibodies (see Table 1), diluted in the blocking solution, were used to soak the slices for 24 h at 4 ℃. After this, all slices were rinsed three times for 10 min in PBS and soaked in the solution with secondary antibodies (see Table 2), which were diluted 1:1000 (in PBS +2% bovine serum albumin), in darkness for 2 h. After washing with PBS three times, the sections were transferred to the surface of glass slides (Langenbrink, Emmendingen, Germany) and mounted in Vectashield Mounting Medium (Vector Laboratories, Burlingame, CA).

The primary antibodies	Solution	Company
Rabbit anti-Iba1	1:500	Wako, VA, USA
Rat anti-CD 68	1:1000	Abd Serotec, Oxfordshire, UK
Mouse anti-TH	1:400	Millipore (MAB 318)
Rabbit anti-NeuN	1:500	Millipore (ABN 78)

Table 1. The list of primary antibodies

The secondary antibodies	Solution	Company
Donkey-anti-mouse IgG-conjugated Alexa Fluor 350	1:1000	Molecular Probes
Donkey-anti-rabbit IgG-conjugated Alexa Fluor 488	1:1000	Molecular Probes
Donkey-anti-rat, IgG-conjugated Alexa Fluor 594	1:1000	Molecular Probes
Donkey-anti-mouse IgG-conjugated Alexa Fluor 594	1:1000	Molecular Probes

Table 2. The list of secondary antibodies

After labelling, slices were imaged with a Nikon 40× water immersion objective

(Nikon 40x, 0.8 NA, Tokyo, Japan) using a zoom factor of ×2.5 and a step size of 1 μm. The Olympus Fluoview 300 laser scanning microscope combined with the MaiTai laser (Spectra-Physics, Mountain View, CA) were used to acquire 3D 2-photon images.

In double-stained sections, an 800 nm wavelength light source was used for the excitation of Alexa Fluor 488 and Alexa Fluor 594. A 585 nm dichroic mirror was used to separate their emitted light, which guided photons, emitted by Alexa Fluor 488, to PMT1 and photons, derived from Alexa Fluor 594, to PMT2. Moreover, to filter the light of impurities, the photons directed to PMT1 were filtered with a 536/40 bandpass filter, and the 568 LP filter was used in front of PMT2.

In triple-stained sections, for accurate localization of SNc and VTA, a 750 nm wavelength light source was used for the excitation of Alexa Fluor 350 and the emitted light was separated by a 515 nm dichroic mirror. Therefore, we can capture the area (SNc or VTA) of dopaminergic neurons stained with Alexa Fluor 350. Then fixed the slides, switched the light source to the wavelength of 800 nm, the rest procedure was the same as described for imaging of double-stained slices.

2.3. Behavioural tests

2.3.1. Stride length

Control mice, as well as mice treated for 9 weeks, were used for behavioural testing. The experimental setup consisted of a bright runway heading towards and ending in a dark box (4.5 cm wide, 40 cm long). After adaptation to the experimental setup, the footprints of experimental animals were recorded after wetting the animals' fore and hind paws with ink and letting them walk on a strip of paper, which was placed on top of the runway.

2.3.2. Open field test

The mice were put in the arena (40×40 cm) and allowed to adapt to the surrounding for 5 minutes. During 10 min, the movement of each mouse was captured by a camera positioned 40 cm above the test arena. The arena was cleaned with 25% alcohol after each test.

2.4. Data analysis and statistics

2.4.1. Statistic analysis for immunofluorescence

Five different fields of view from immunolabeled brain slices were acquired from each brain region of each mouse. The number of neurons was determined manually using Image J software, the boundary between SNc and SNr was defined by the difference in neuronal number, the region where the scattered neurons are present is regarded as SNr, the cells at the boundary of images were excluded for counting. The statistical analysis was performed on GraphPad. Box-and-whisker plots show 25^{th} and 75^{th}, whiskers 10^{th} and 90^{th} percentiles. For comparison of multiple data sets, the Kruskal-Wallis test followed by the post-hoc Dunn's correction was carried out. For comparison of two data sets, the Mann-Whitney test was used, the compared groups were considered to be statistically different if p-values were below 0.05. The Kolmogorov-Smirnov test was performed for comparing data distributions, the compared curves were taken as statistically different if p-values were below 0.05.

2.4.2. Statistic analysis for behavioural tests

The data for the stride length and base width were analyzed by measuring the distance between the two consecutive steps of the same paw and the distance between the right and left paw, respectively.

For analysis of the open field test (OFT), the videos were imported into Image J, the plugin named "mmtracking" with the setting of the gray threshold 0-60 was used. This ensured that the tracks of mice covered all the bodies except the tail. All tracking information was obtained in sequential order, all continuous tracking points were drawn within the coordinate system (X-axis range from 80 or 90 to 160 or 170; Y-axis range from 0 to 120) to present respective continuous curves. The distance to each successive point was calculated by the Pythagorean Theorem. To obtain the distance and duration of the mouse movement in the central field, we set the coordinate range X-axis 100 (110)-140 (150) and Y-axis 30-90 in the Excel table (25% in the total surface area), so that the data in the central area were screened out. Thereby, the total distance moved in

the entire arena, as well as the distance and duration in the central area were measured. Box-and-whisker plots show 25^{th} and 75^{th}, whiskers 10^{th} and 90^{th} percentiles, Kruskal-Wallis test followed by the post-hoc Dunn's correction was performed for the comparison of multiple data sets. The differences between the compared groups were regarded as significant if p-values were below 0.05.

3. Results

To assess the association between liver damage and histological and behavioural hallmarks of Parkinsonism, the mice were intraperitoneally (i.p.) injected with CCl4 to induce liver damage and inflammation response. We investigated 3 different phases of CCl4-induced liver damage: acute inflammatory reaction (36 h after a single injection); mild liver fibrosis (after 4 weeks of treatment); severe fibrosis (after 9 weeks of treatment). After treatment, the brain tissue was isolated for immunohistochemical analysis.

3.1. Significant loss of neurons in the SNc, not in the VTA, of mice with mild fibrosis

First, we analyzed the overall neuronal density as well as the density of dopaminergic and non-dopaminergic cells in the VTA of mice, treated over 4 weeks (i.p. injections twice per week) with 0.9% NaCl (Control), oil (Vehicle), or CCl4 dissolved in oil (0.4 µl/g). To do so, coronal brain sections (50 µm thick) were stained with an anti-NeuN antibody for visualization of neurons and an anti-TH antibody for visualization of dopaminergic neurons. There was no significant difference in the density of TH^+, TH^- or $NeuN^+$ neurons in the VTA (Fig. 2; $p > 0.05$; Kruskal-Wallis test followed by post-hoc Dunn's correction, n = 4-5 mice per group, 5 areas per mouse).

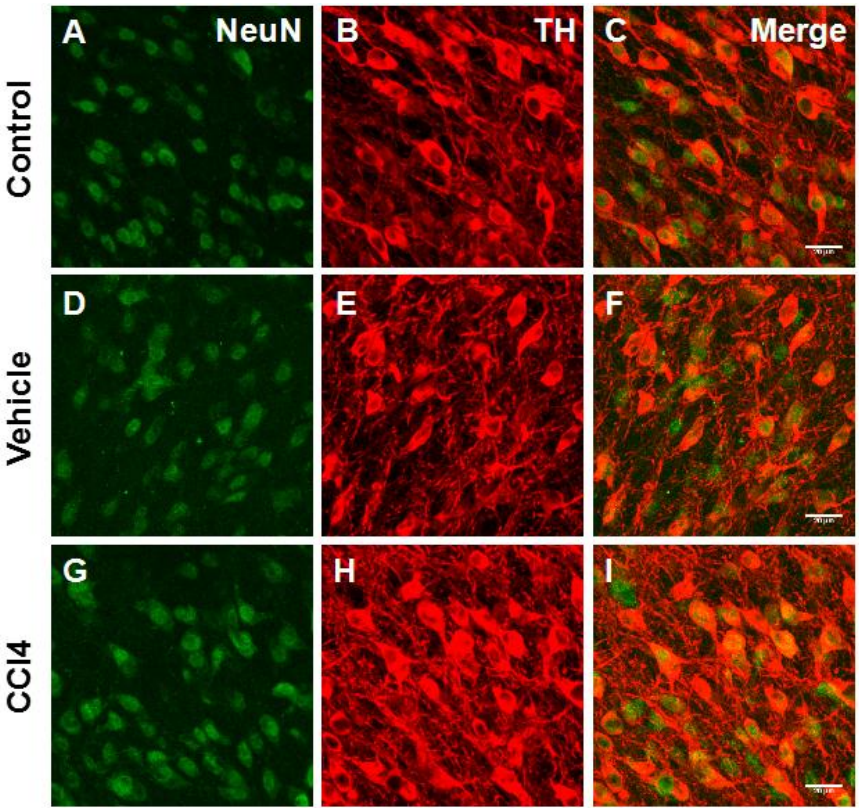

Figure 1. No apparent loss of neurons in the VTA of mice with mild liver fibrosis. Maximum-intensity projection (MIP) images (1-20 μm depth) of fixed brain slices of mice injected i.p. with 0.9% NaCl (Control), oil (Vehicle), or CCl4 dissolved in oil (0.4 μl/g) two times per week over 4 weeks. Coronal brain sections were stained with an anti-NeuN antibody for visualization of neurons (green: A, D, G) and an anti-TH antibody for visualization of dopaminergic neurons (red: B, E, H). The merged images are shown in C, F, and I. Scale bar, 20 μm.

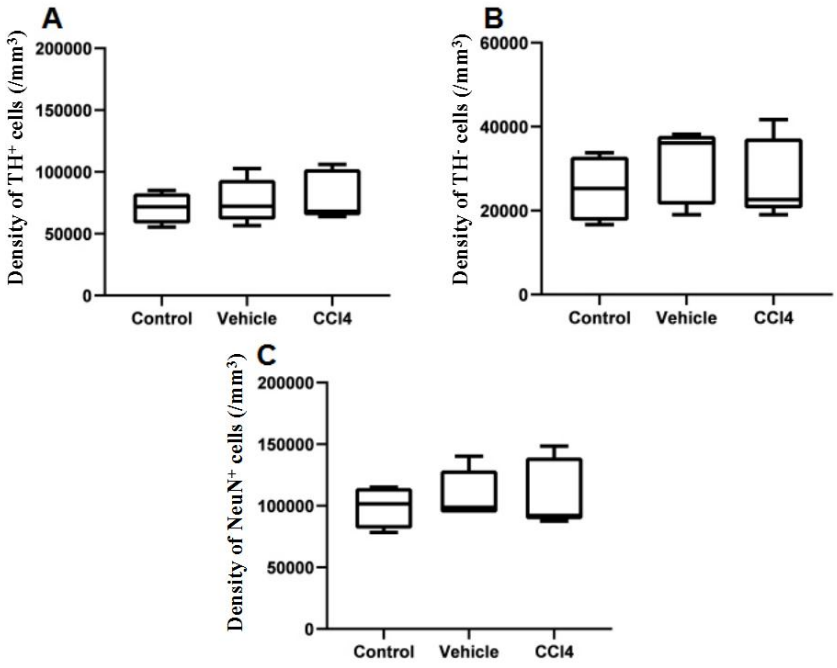

Figure 2. Mild liver fibrosis does not affect the neuronal density in the VTA. Box-and-whisker plots showing the median (per mouse) density of TH^+ dopaminergic neurons (A), TH^- neurons (B) and any neurons (C) in mice injected i.p. with 0.9% NaCl (Control, n = 4 mice), oil (Vehicle, n = 5 mice), or CCl4 (n = 5 mice) dissolved in oil (0.4 µl/g) two times per week over 4 weeks. There was no significant difference in the density of TH^+, TH^- or $NeuN^+$ neurons in the VTA ($p > 0.05$; Kruskal-Wallis test followed by post-hoc Dunn's correction, n = 4-5 mice per group, 5 areas per mouse).

Next, we analyzed the overall neuronal density as well as the density of dopaminergic and non-dopaminergic cells in the SNc. We used the same staining protocol, and the SNc was identified base on its higher neuronal density (NeuN channel) compared to SNr. (Fig. 3).

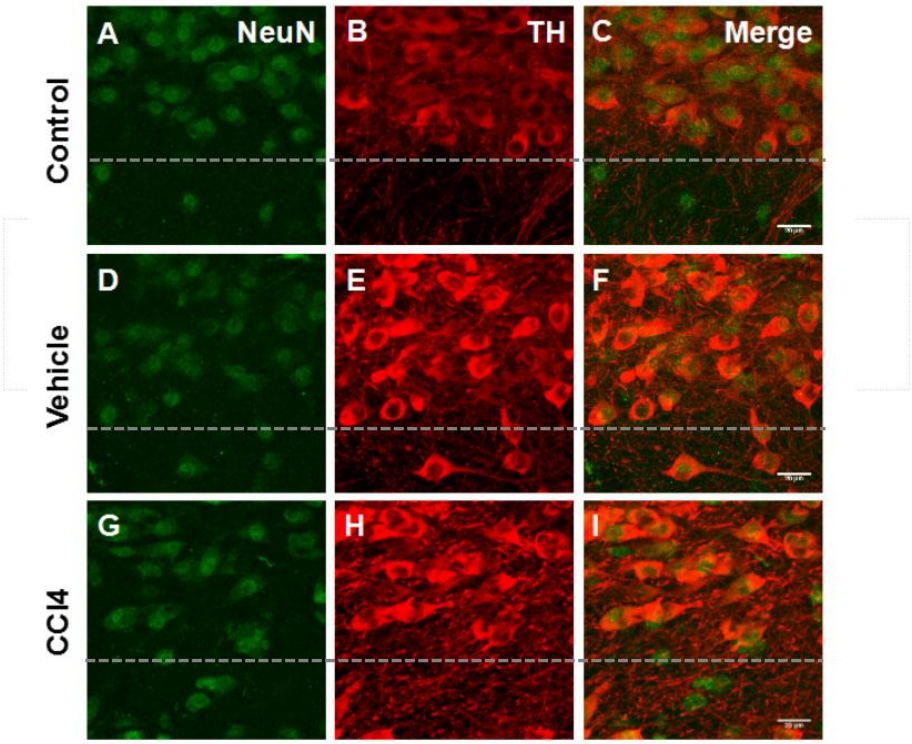

Figure 3. Significant loss of neurons in the SNc of mice with mild fibrosis. MIP images (1-20 µm depth) of fixed brain slices of mice injected i.p. with 0.9% NaCl (Control), oil (Vehicle), or CCl4 dissolved in oil (0.4 µl/g) two times per week over 4 weeks. Coronal brain sections were stained with an anti-NeuN antibody for visualization of neurons (green: A, D, G) and an anti-TH antibody for visualization of dopaminergic neurons (red: B, E, H). The merged images are shown in C, F, and I. The grey dotted line serves as the dividing line between SNc and SNr. Scale bar, 20 µm.

Interestingly, there was a significant decrease (by nearly 40%) in the density of

TH^+ neurons in the SNc of mice treated with CCl4, when compared to the mice treated with 0.9% NaCl or oil (Fig. 4; *p = 0.03 for both comparisons; Kruskal-Wallis test followed by post-hoc Dunn's correction, n = 4-5 mice per group, 5 areas per mouse). There was no significant difference in the density of TH^- or $NeuN^+$ neurons in the SNc (Fig. 4; p > 0.05; Kruskal-Wallis test followed by post-hoc Dunn's correction). In this case, it seems to mean the loss of TH^+ cells instead of a decrease in expression of TH in cells in SNc.

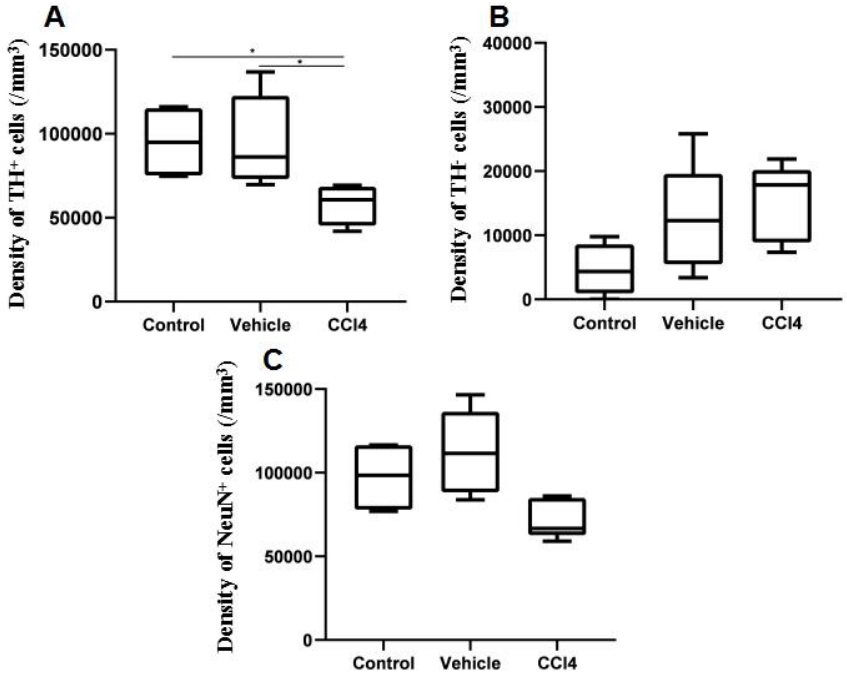

Figure 4. Mild liver fibrosis does affect the neuronal density in the SNc. Box-and-whisker plots showing the median (per mouse) density of TH^+ dopaminergic neurons (A), TH^- neurons (B) and any neurons (C) in mice injected i.p. with 0.9% NaCl (Control, n = 4 mice), oil (Vehicle, n = 5 mice), or CCl4 (n = 5 mice) dissolved in oil (0.4 µl/g) two times per week over 4 weeks. There was a significant decrease in the density of TH^+ neurons in the SNc of mice treated with CCl4 when compared to the mice treated with 0.9% NaCl and oil (*p = 0.03 for both comparisons; Kruskal-Wallis test followed by post-hoc Dunn's correction, n = 4-5 mice per group, 5 areas per mouse). There was no significant difference in the density of TH^- or $NeuN^+$ neurons in the SNc (p > 0.05; Kruskal-Wallis test followed by post-hoc Dunn's correction).

These results indicated that CCl4-induced neurotoxicity causes a moderate but significant loss of dopaminergic neurons in the SNc but not in the VTA. This is consistent with the literature data describing the higher vulnerability of neurons in the SNc (Surmeier et al. 2017). However, the underlying mechanism remains unclear.

3.2. Mild liver fibrosis is not accompanied by ongoing microglial activation

Because of the loss of neurons in the SNc in mice with mild fibrosis, we asked whether this might be a consequence of the pronounced activation of microglia in the SN or other regions of the brain. As a readout for microglial activation, we calculated the density of microglial cells as well as the microglial soma size, which both are known to be increased under conditions of microglial activation. Furthermore, the fluorescence intensity of the microglial activation marker Iba-1, as well as the phagocytosis marker CD 68, were analyzed. As shown in Fig. 5, There was no obvious change of microglial morphology in the SNr of mice with mild fibrosis.

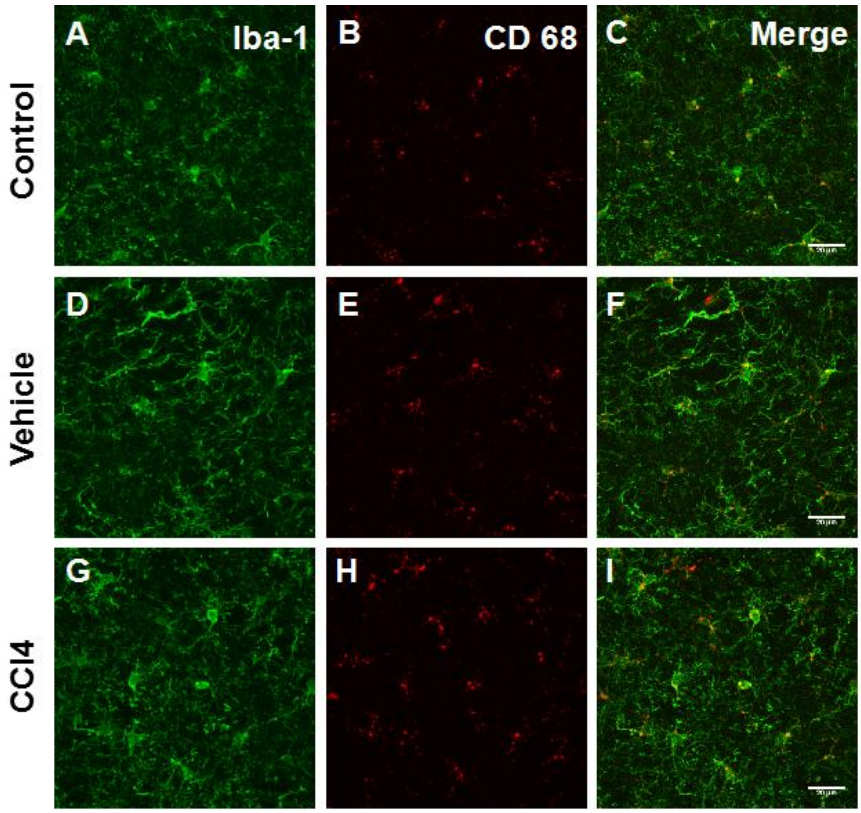

Figure 5. No apparent change in microglial morphology in the SNr of mice with mild fibrosis. MIP images (1-40 µm depth) of fixed brain slices of mice injected i.p. with 0.9% NaCl (Control), oil (Vehicle), or CCl4 dissolved in oil (0.4 µl/g) two times per week over 4 weeks. Coronal brain sections were stained with an anti-Iba-1 antibody for visualization of microglia (green: A, D, G) and an anti-CD 68 antibody for visualization of phagocytic activity of microglia (red: B, E, H). The merged images are shown in C, F, and I. Scale bar, 20 µm.

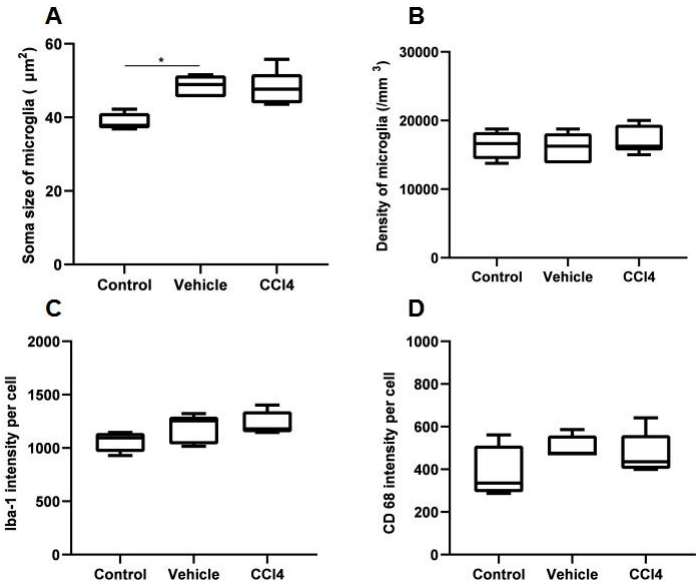

Figure 6. Mild liver fibrosis does not cause microglial activation in the SNr. Box-and-whisker plots showing the median (per mouse) soma size (A), density (B), Iba-1 (C) and CD 68 (D) fluorescence intensity of microglia in mice injected i.p. with 0.9% NaCl (Control, n = 4 mice), oil (Vehicle, n = 5 mice), or CCl4 (n = 5 mice) dissolved in oil (0.4 µl/g) two times per week over 4 weeks. There was a significant increase in the soma size of microglia in the SNr of mice treated with oil when compared to the mice treated with 0.9% NaCl (*p = 0.02; Kruskal-Wallis test followed by post-hoc Dunn's correction, n = 4-5 mice per group, 5 areas per mouse). There was no significant difference in the soma size of microglia in the SNr of mice treated with CCl4 when compared to the mice treated with 0.9% NaCl and oil (p > 0.05 for both comparisons; Kruskal-Wallis test followed by post-hoc Dunn's correction). Besides, there was no significant difference in the density of microglia and the intensity of Iba-1 and CD 68 in the SNr (p > 0.05; Kruskal-Wallis test followed by post-hoc Dunn's correction).

As shown in Fig. 6, there was a meaningful increase in the soma size of microglia in the SNr of mice treated with oil when compared to the mice treated with 0.9% NaCl (*p = 0.02; Kruskal-Wallis test followed by post-hoc Dunn's correction, n = 4-5 mice per group, 5 areas per mouse), suggesting that oil itself can induce an increase of the soma size of microglia. However, there was no significant difference in the soma size of microglia between the oil and the CCl4 groups (p > 0.05; Kruskal-Wallis test followed by post-hoc Dunn's correction). Besides, there was no significant difference in the density of microglia and the intensity of Iba-1 and CD 68 in the SNr (p > 0.05; Kruskal-Wallis test followed by post-hoc Dunn's correction).

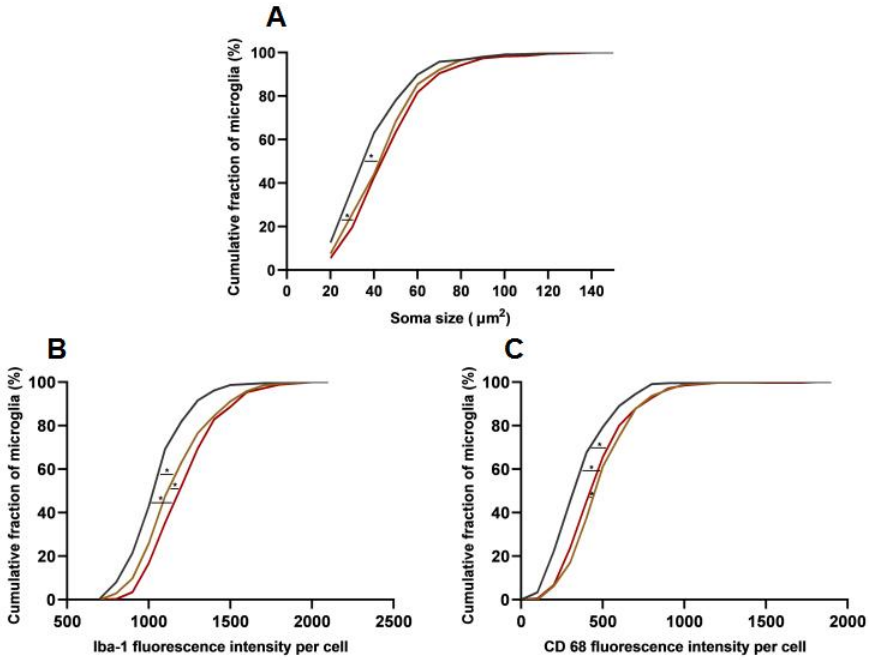

Figure 7. Moderate changes of microglial soma size, as well as Iba-1 and CD 68 fluorescence in the SNr. Cumulative probability function illustrating the distributions (per cell) of the soma size (A) as well as Iba-1 (B) and CD 68 (C) intensity in the SNr of mice, injected i.p. with 0.9% NaCl (Control, black curve), oil (Vehicle, yellow curve), or CCl4 (red curve) dissolved in oil (0.4 µl/g) two times per week over 4 weeks (Control: n = 238 cells from 4 mice, Vehicle: n = 317 cells from 5 mice, CCl4: n = 345 cells from 5 mice). The distributions of the soma size in mice treated with vehicle or CCl4 were significantly shifted to the right when compared to the control group (*p < 0.05 for both comparisons, Kolmogorov-Smirnov test), and a similar tendency was seen in the distributions of Iba-1 and CD 68 intensities (*p < 0.05 for all comparisons, Kolmogorov-Smirnov test). There was no significant difference in the distributions of soma size between mice treated with oil and CCl4 (p > 0.05, Kolmogorov-Smirnov test), whereas the distribution of Iba-1 fluorescence intensity was shifted to the right in mice treated with CCl4 when compared to the mice treated with oil (*p < 0.05, Kolmogorov-Smirnov test). In contrast, the distribution of CD 68 fluorescence intensity was shifted to the left in mice treated with CCl4 when compared to the mice treated with oil (*p = 0.02, Kolmogorov-Smirnov test).

To analyze the changes of microglia in the SNr in more detail, we plotted the cumulative distributions of the soma size, as well as Iba-1 and CD 68 fluorescence (Figure 7; Control: n = 238 cells from 4 mice, Vehicle: n = 317 cells from 5 mice, CCl4: n = 345 cells from 5 mice). The distributions of soma size in mice treated with vehicle or CCl4 was significantly shifted to the right when compared to the control group (*p < 0.05 for both comparisons, Kolmogorov-Smirnov test), and a similar tendency was seen in the distributions of Iba-1 and CD 68 intensities (*p < 0.05 for all comparisons, Kolmogorov-Smirnov test). There was no significant difference in the distributions of

soma size between mice treated with oil and CCl4 ($p > 0.05$, Kolmogorov-Smirnov test), whereas the distribution of Iba-1 fluorescence intensity was shifted to the right in mice treated with CCl4 when compared to the mice treated with oil (*$p < 0.05$, Kolmogorov-Smirnov test). In contrast, the distribution of CD 68 fluorescence intensity was shifted to the left in mice treated with CCl4 when compared to the mice treated with oil (*$p = 0.02$, Kolmogorov-Smirnov test). These data suggest that indeed, the vehicle induces a slight activation of microglia in the SNr.

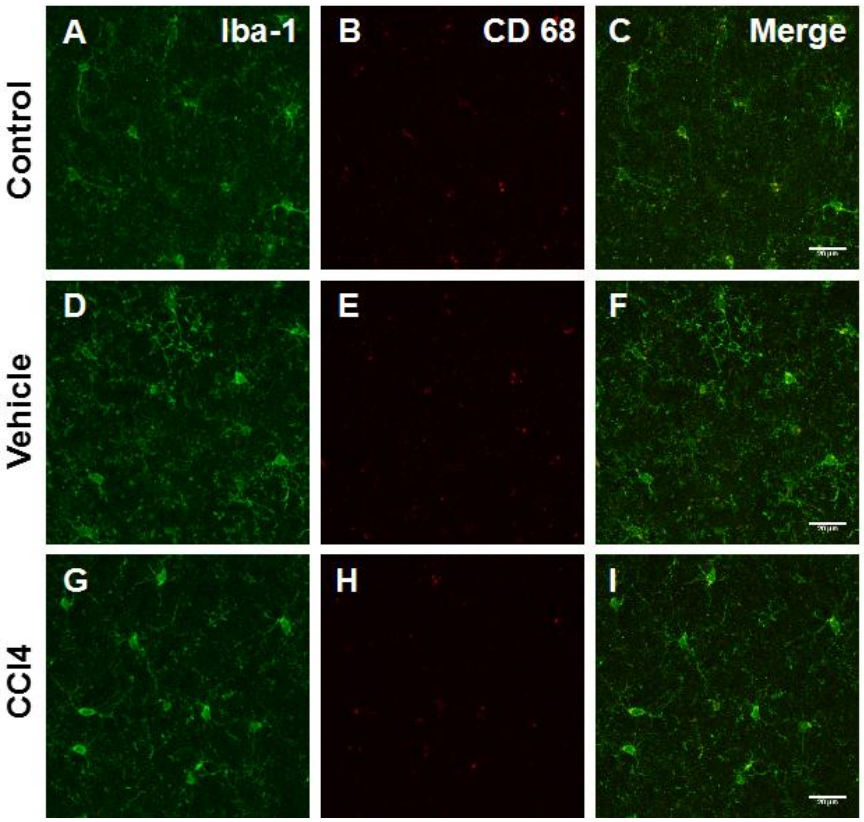

Figure 8. No apparent morphological change of microglia in the cerebral cortex of mice with mild fibrosis. MIP images (1-40 µm depth) of fixed cortical slices of mice injected i.p. with 0.9% NaCl (Control), oil (Vehicle), or CCl4 dissolved in oil (0.4 µl/g) two times per week over 4 weeks. Coronal brain sections were stained with an anti-Iba-1 antibody for visualization of microglia (green: A, D, G) and an anti-CD 68 antibody for visualization of phagocytic activity of microglia (red: B, E, H). The merged images are shown in C, F, and I. Scale bar, 20 µm.

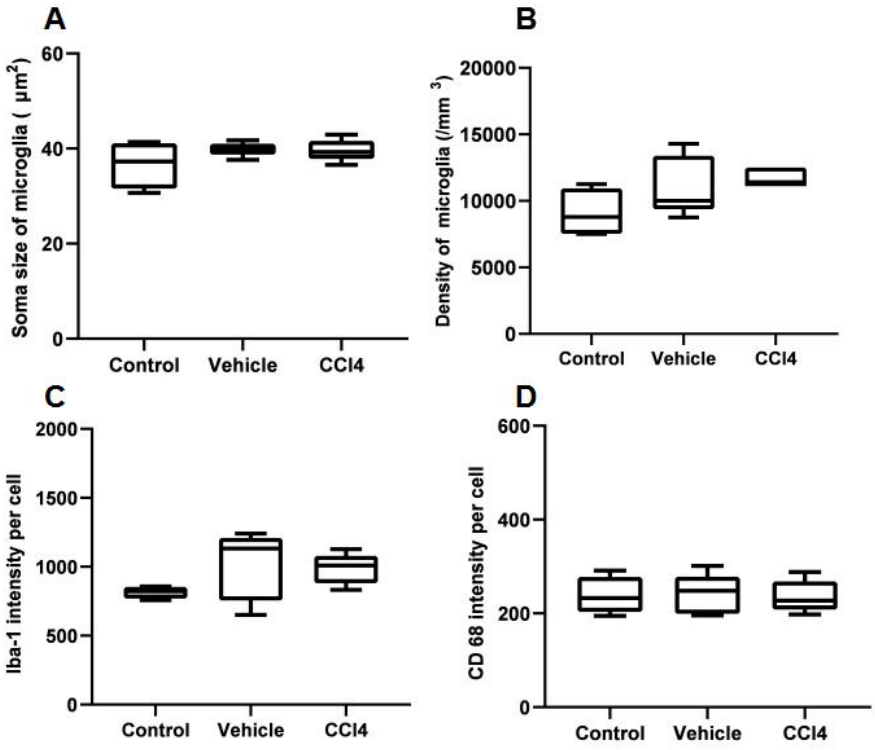

Figure 9. Mild liver fibrosis does not cause any microglial activation in the cerebral cortex. Box-and-whisker plots showing the median (per mouse) soma size (A), density (B), Iba-1 (C) and CD 68 (D) fluorescence intensity of microglia in mice injected i.p. with 0.9% NaCl (Control, n = 4 mice), oil (Vehicle, n = 5 mice), or CCl4 (n = 5 mice) dissolved in oil (0.4 µl/g) two times per week over 4 weeks. There was no significant difference in the soma size, density, the Iba-1 and CD 68 fluorescence intensity of microglia in the cerebral cortex($p > 0.05$ for all comparisons; Kruskal-Wallis test followed by post-hoc Dunn's correction, n = 4-5 mice per group, 5 areas per mouse).

To check microglial activation in other areas of the brain, we analyzed the microglial morphology in the cerebral cortex. We used the same staining and imaging protocols as those described above were performed as. There was no apparent change of microglial morphology in the cerebral cortex of mice with mild fibrosis (Fig. 8, 9).

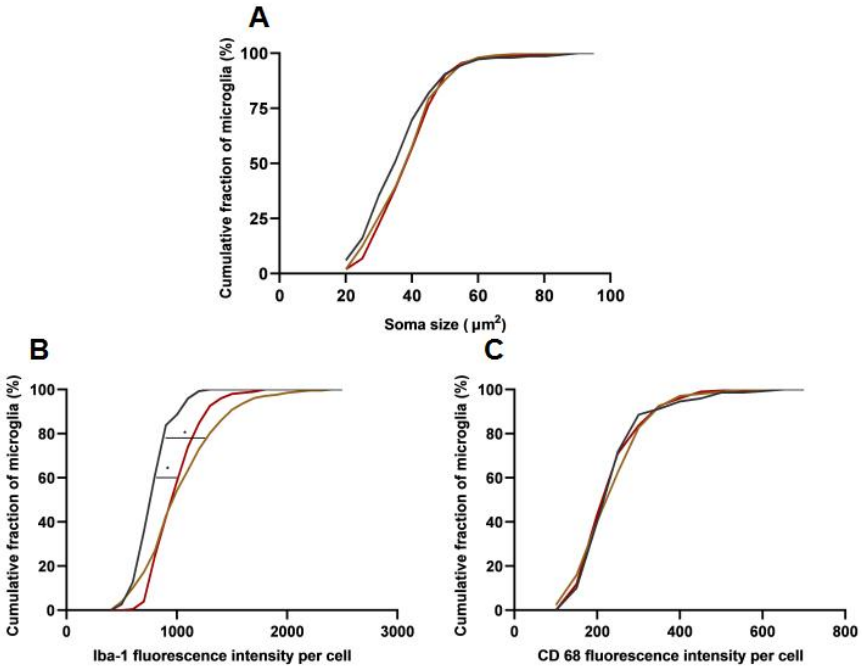

Figure 10. Small but significant changes of soma size of cortical microglia. Cumulative probability functions illustrating the distributions (per cell) of soma size (A) as well as Iba-1 (B) and CD 68 (C) fluorescence intensity in the cortex of mice injected i.p. with 0.9% NaCl (Control, black curve), oil (Vehicle, yellow curve), or CCl4 (red curve) dissolved in oil (0.4 µl/g) two times per week over 4 weeks (Control: n = 149 cells from 4 mice, Vehicle: n = 208 cells from 5 mice, CCl4: n = 204 cells from 5 mice). The distributions of soma size in mice treated with vehicle or CCl4 were slightly but not significantly shifted to the right ($p > 0.05$ for both comparisons, Kolmogorov-Smirnov test), the distribution of Iba-1 fluorescence intensity in mice treated with vehicle or CCl4 was shifted to the right significantly when compared to the control group (*$p < 0.05$ for both comparisons, Kolmogorov-Smirnov test). There was no significant difference in the distribution of CD 68 fluorescence intensities in all three groups ($p > 0.05$, Kolmogorov-Smirnov test).

Similarly, the distributions (per cell) of soma size and CD 68 fluorescence intensities showed no difference between all the groups (Fig. 10; Control: n = 149 cells from 4 mice, Vehicle: n = 208 cells from 5 mice, CCl4: n = 204 cells from 5 mice; $p > 0.05$ for all comparisons, Kolmogorov-Smirnov test). However, Iba-1 fluorescence increased in vehicle- or CCl4- treated mice when compared to Control mice, again suggesting a slight activation of microglia by vehicle-treatment (Fig. 10; Control: n = 149 cells from 4 mice, Vehicle: n = 208 cells from 5 mice, CCl4: n = 204 cells from 5 mice; *$p < 0.05$ for both comparisons, Kolmogorov-Smirnov test).

These results reveal that the vehicle itself slightly changes the microglial morphology, but the CCl4 treatment does not have any additional effect at this time

point. Besides, the changes in microglia in SNr were more pronounced than those in cortical microglia.

3.3. Selective and significant loss of neurons in the SNc of mice with severe fibrosis

To explore whether neuronal loss increases with the severity of liver pathology, we repeated the described above experiments in mice treated with CCl4 for a prolonged period (9 weeks)(Fig. 11). Under this treatment there was no significant difference in the density of TH^+, TH^- or $NeuN^+$ neurons in the VTA (Fig. 12; $p > 0.05$; Kruskal-Wallis test followed by post-hoc Dunn's correction, n = 4-7 mice per group, 5 areas per mouse).

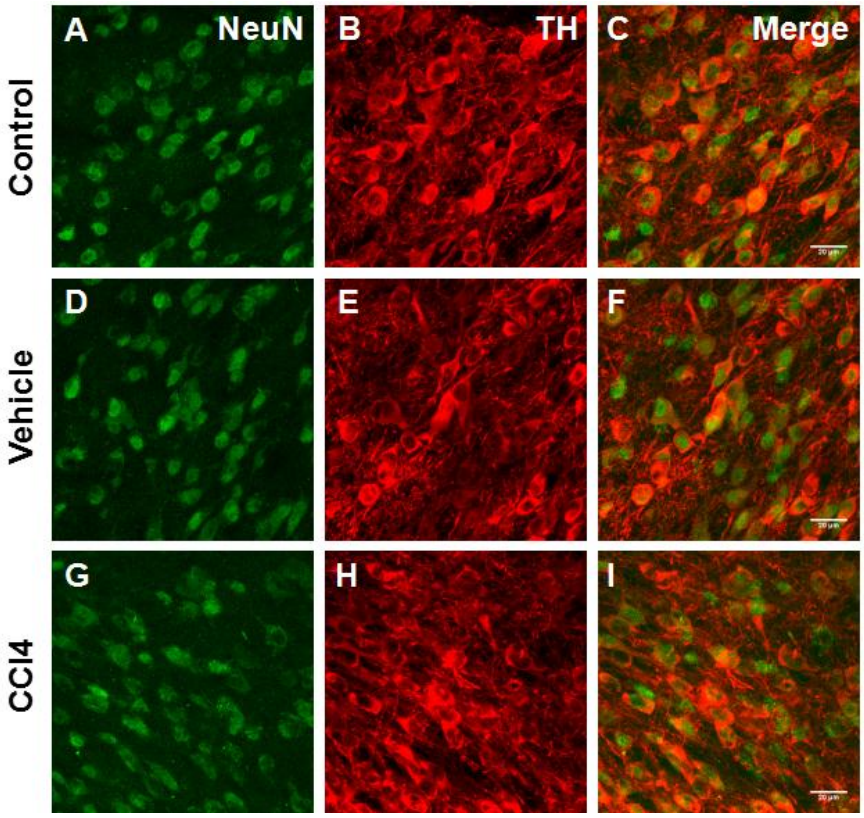

Figure 11. No apparent loss of neurons in the VTA of mice with severe fibrosis. MIP images (1-20 µm depth) of fixed brain slices of mice injected i.p. with 0.9% NaCl (Control), oil (Vehicle), or CCl4 dissolved in oil (0.4 µl/g) two times per week over 9 weeks. Coronal brain sections were stained with an anti-NeuN antibody for visualization of neurons (green: A, D, G) and an anti-TH antibody for visualization of dopaminergic neurons (red: B, E, H). The merged images are shown in C, F, and I. Scale bar, 20 µm.

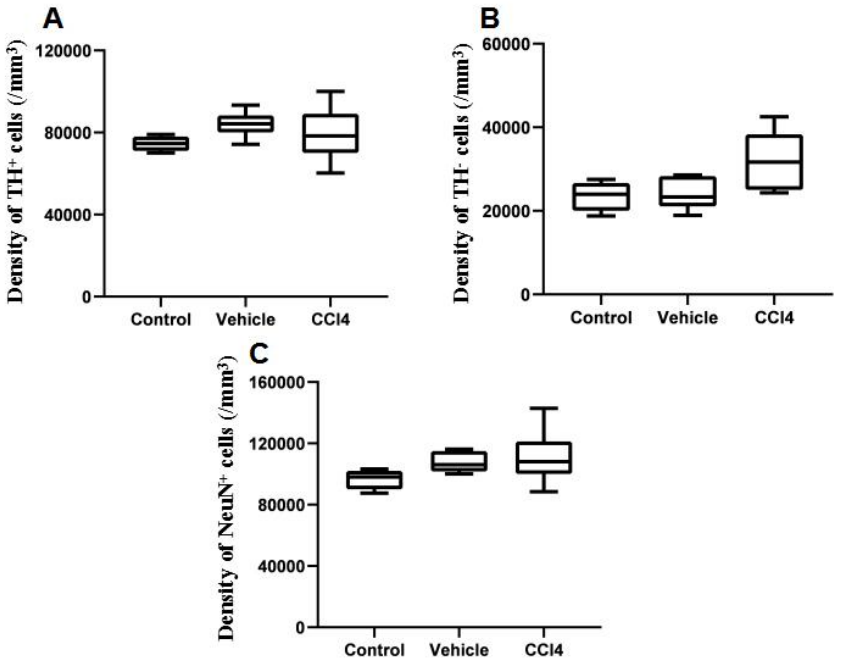

Figure 12. Severe liver fibrosis does not affect the neuronal density in the VTA. Box-and-whisker plots showing the median (per mouse) density of TH^+ dopaminergic neurons (A), TH^- neurons (B), and any neurons (C) in mice injected i.p. with 0.9% NaCl (Control, n = 4 mice), oil (Vehicle, n = 7 mice), or CCl4 (n = 7 mice) dissolved in oil (0.4 μl/g) two times per week over 9 weeks. There was no significant difference in the density of TH^+, TH^- or $NeuN^+$ neurons in the VTA ($p > 0.05$; Kruskal-Wallis test followed by post-hoc Dunn's correction, n = 4-7 mice per group, 5 areas per mouse).

However, similar analyses of the SNc showed a remarkable loss of neurons (Fig. 13). We used the same way of calculation as described above to analyze the density of neurons in SNc. As shown in Fig. 14, there was a significant (nearly 30%) decrease in the density of TH^+ and $NeuN^+$ neurons in the SNc of mice treated with CCl4 when compared to the mice treated with oil (*$p < 0.05$ for both comparisons; Kruskal-Wallis test followed by post-hoc Dunn's correction, n = 4-7 mice per group, 5 areas per mouse).

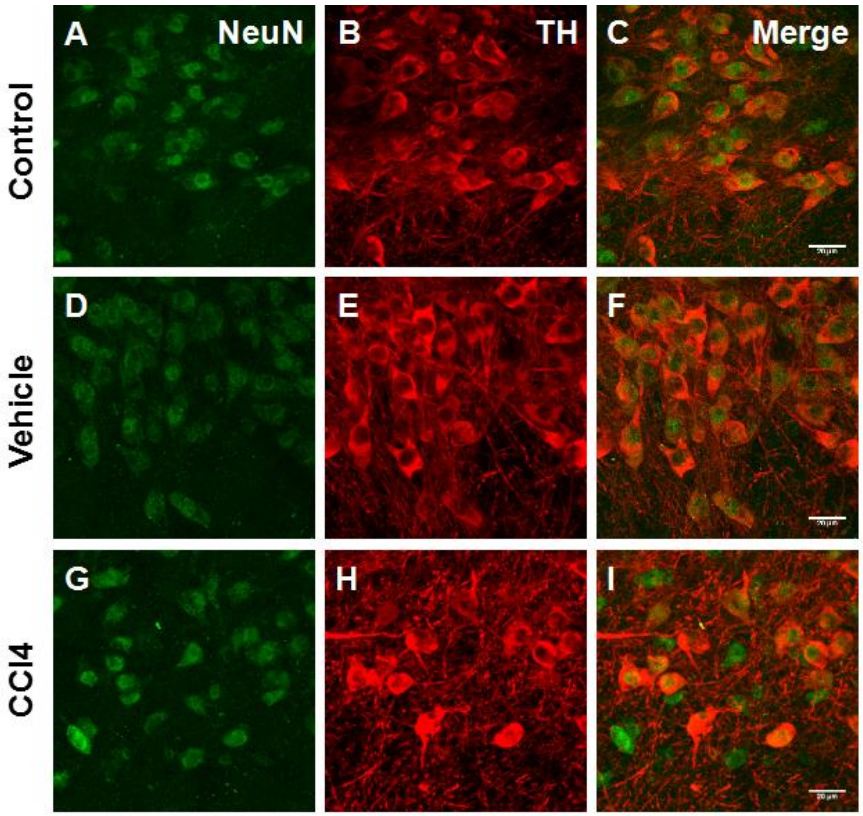

Figure 13. Significant loss of neurons in the SNc of mice with severe fibrosis. MIP images (1-20 µm depth) of fixed brain slices of mice injected i.p. with 0.9% NaCl (Control), oil (Vehicle), or CCl4 dissolved in oil (0.4 µl/g) two times per week over 9 weeks. Coronal brain sections were stained with an anti-NeuN antibody for visualization of neurons (green: A, D, G) and an anti-TH antibody for visualization of dopaminergic neurons (red: B, E, H). The merged images are shown in C, F, and I. Scale bar, 20 µm.

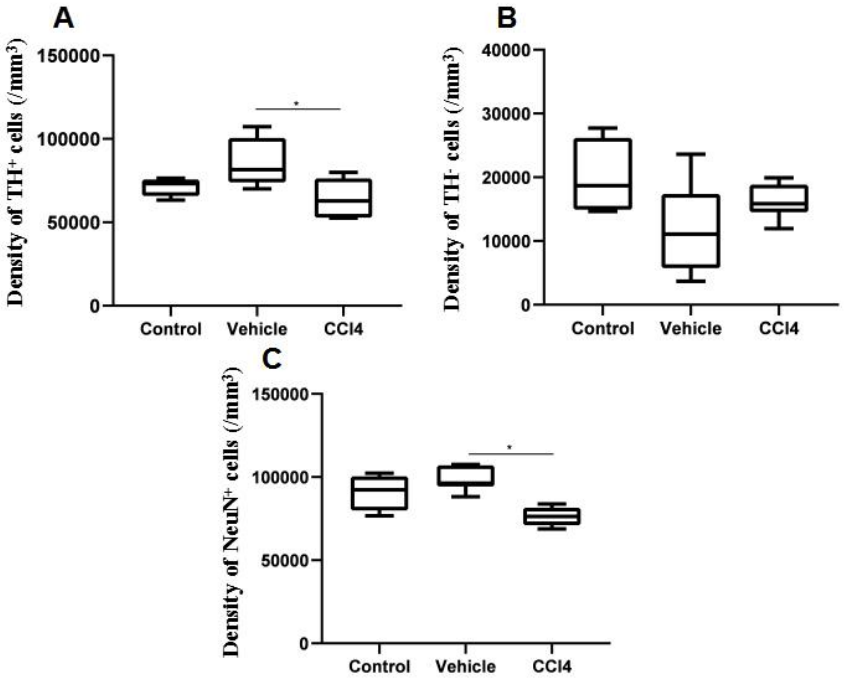

Figure 14. Severe liver fibrosis decreases neuronal density in the SNc. Box-and-whisker plots showing the median (per mouse) density of TH^+ dopaminergic neurons (A), TH^- neurons (B), and any neurons (C) in mice injected i.p. with 0.9% NaCl (Control, n = 4 mice), oil (Vehicle, n = 7 mice), or CCl4 (n = 7 mice) dissolved in oil (0.4 µl/g) two times per week over 9 weeks. There was a significant decrease in the density of TH^+ and $NeuN^+$ neurons in the SNc of mice treated with CCl4 when compared to mice treated with oil (*p = 0.01, *p = 0.002 respectively; Kruskal-Wallis test followed by post-hoc Dunn's correction, n = 4-7 mice per group, 5 areas per mouse).

These results substantiated the finding that CCl4-induced neurotoxicity causes selective loss of neurons in the SNc but not in the VTA. The extent of neuron loss caused by mild fibrosis reached 40%, while the number of neurons lost during severe fibrosis was almost the same (30%).

3.4. Severe liver fibrosis is not accompanied by microglial activation

Under conditions of severe fibrosis, the parameters of microglial activation were analyzed in VTA and SNr, similar to data obtained in mice with mild fibrosis. Also, microglial properties were analyzed in the SNc, the region where the neuronal loss occurred.

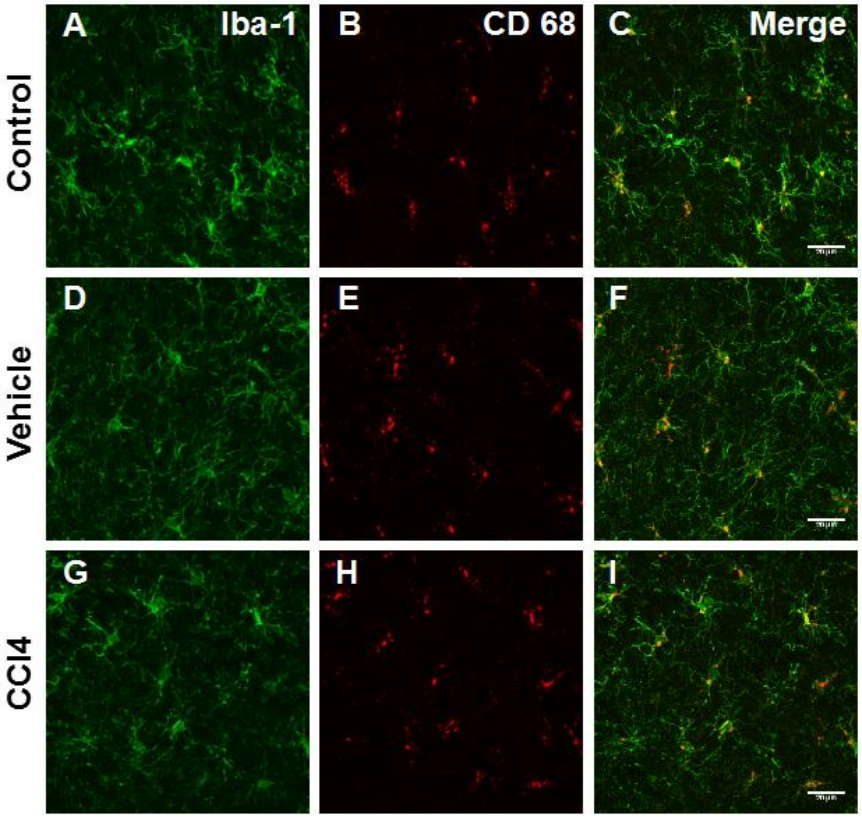

Figure 15. No apparent morphological change of microglia in the SNr of mice with severe fibrosis. MIP images (1-30 µm depth) of fixed brain slices of mice injected i.p. with 0.9% NaCl (Control), oil (Vehicle), or CCl4 dissolved

in oil (0.4 µl/g) two times per week over 9 weeks. Coronal brain sections were stained with an anti-Iba-1 antibody for visualization of microglia (green: A, D, G) and an anti-CD 68 antibody for visualization of phagocytic activity of microglia (red: B, E, H). The merged images are shown in C, F, and I. Scale bar, 20 µm.

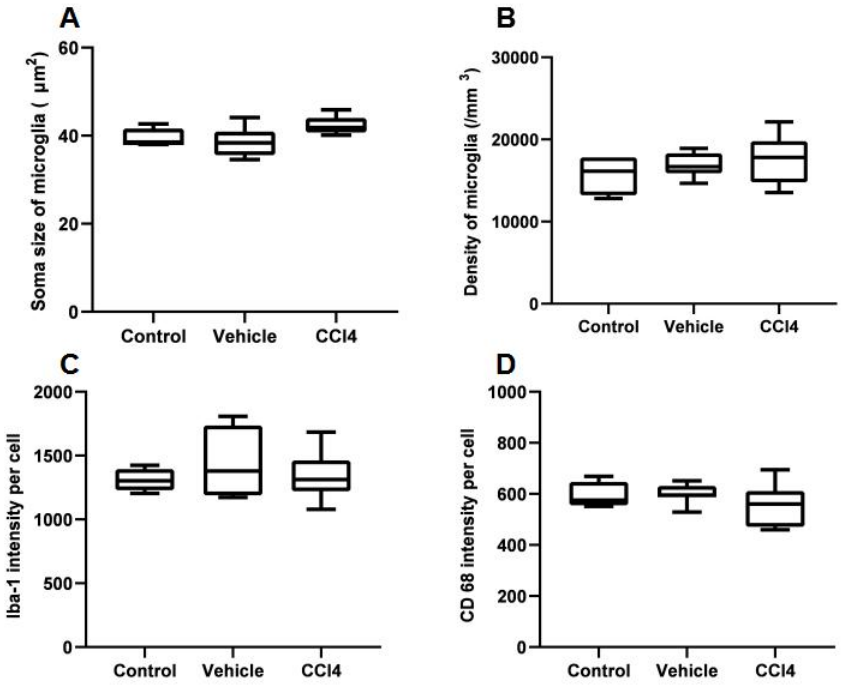

Figure 16. Severe liver fibrosis does not cause microglial activation in the SNr. Box-and-whisker plots showing the median (per mouse) soma size (A), density (B), Iba-1 (C) and CD 68 (D) fluorescence intensity of microglia in mice injected i.p. with 0.9% NaCl (Control, n = 4 mice), oil (Vehicle, n = 7 mice), or CCl4 (n = 7 mice) dissolved in oil (0.4 µl/g) two times per week over 9 weeks. There was no significant difference in the soma size, density, the Iba-1 and CD 68 fluorescence intensity of microglia in the SNr ($p > 0.05$ for all comparisons; Kruskal-Wallis test followed by post-hoc Dunn's correction, n = 4-7 mice per group, 5 areas per mouse).

Similar to the result from mild fibrosis, there was no apparent morphological change of microglia in the SNr of mice with severe fibrosis (Fig. 15). There was no significant difference in the median (per mouse) soma size, density, the Iba-1 and CD 68 fluorescence intensity of microglia in the SNr (Fig. 16; $p > 0.05$ for all comparisons; Kruskal-Wallis test followed by post-hoc Dunn's correction, Control, n = 4 mice, Vehicle, n = 7 mice, CCl4, n = 7 mice, 5 areas per mouse).

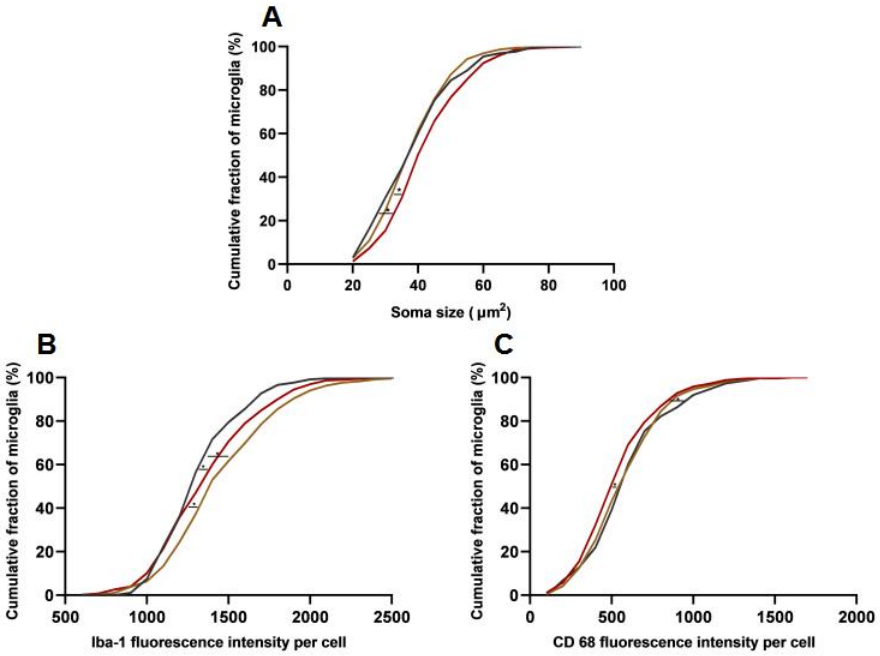

Figure 17. Moderate changes of microglial soma size, as well as Iba-1 and CD 68 fluorescence in the SNr. Cumulative probability function illustrating the distributions (per cell) of soma size (A) as well as Iba-1 (B) and CD 68 (C) fluorescence intensity in the SNr of mice injected i.p. with 0.9% NaCl (Control, black curve), oil (Vehicle, yellow curve), or CCl4 (red curve) dissolved in oil (0.4 µl/g) two times per week over 9 weeks (Control: n = 264 cells from 4 mice, Vehicle: n = 525 cells from 7 mice, CCl4: n = 533 cells from 7 mice). The distribution of soma size in mice treated with CCl4 was significantly shifted to the right when compared to the control and vehicle groups (*p < 0.05 for both comparisons, Kolmogorov-Smirnov test), There was no significant difference in the distributions of soma size between control and vehicle groups (p > 0.05, Kolmogorov-Smirnov test). The distribution of Iba-1 fluorescence intensity was shifted to the right in mice treated with oil or CCl4 when compared to the mice treated with saline (*p < 0.05, Kolmogorov-Smirnov test). In contrast, the distribution of CD 68 fluorescence intensity was shifted to the left in mice treated with CCl4 when compared to the mice treated with saline and oil (*p < 0.05 for both comparisons, Kolmogorov-Smirnov test).

At the level of individual cells (Fig. 17), the distribution of soma size in mice treated with CCl4 was significantly shifted to the right when compared to the control and vehicle groups (*p < 0.05 for both comparisons, Kolmogorov-Smirnov test), there was no significant difference in the distributions of soma size between control and vehicle groups (p > 0.05, Kolmogorov-Smirnov test). The distribution of Iba-1 fluorescence intensity was shifted to the right in mice treated with oil or CCl4 when compared to the mice treated with saline (*p < 0.05, Kolmogorov-Smirnov test). In contrast, the distribution of CD 68 fluorescence intensity was shifted to the left in mice

treated with CCl4 when compared to the mice treated with saline or oil (*$p < 0.05$ for both comparisons, Kolmogorov-Smirnov test).

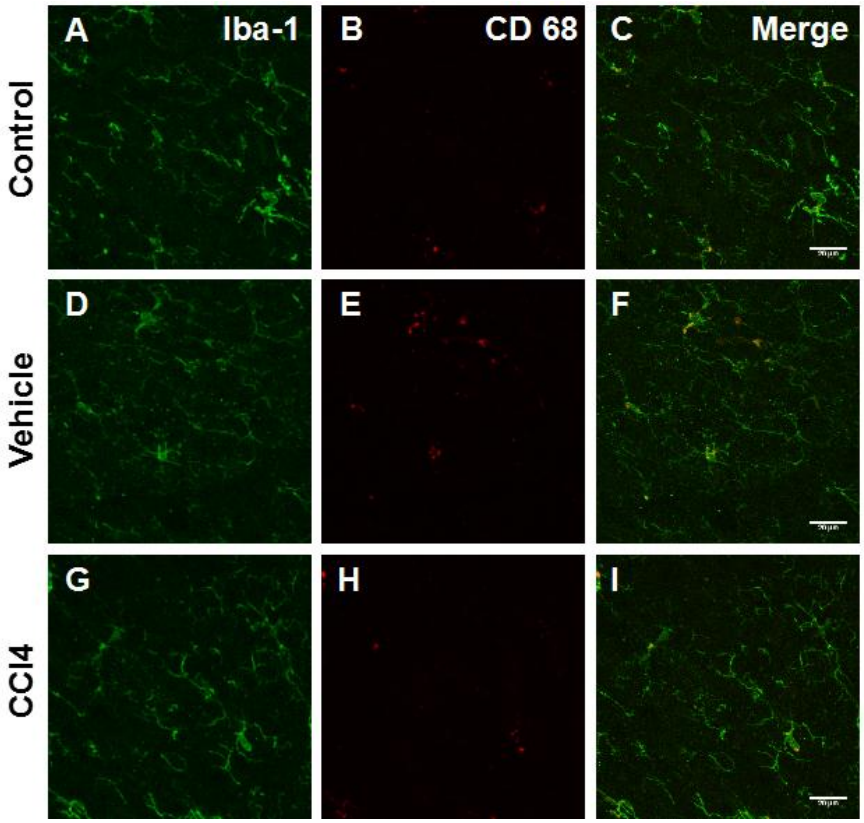

Figure 18. No apparent morphological change of microglia in the VTA of mice with severe fibrosis. MIP images (1-30 μm depth) of fixed brain slices of mice injected i.p. with 0.9% NaCl (Control), oil (Vehicle), or CCl4 dissolved in oil (0.4 μl/g) two times per week over 9 weeks. Coronal brain sections were stained with an anti- Iba-1 antibody for visualization of microglia (green: A, D, G) and an anti-CD 68 antibody for visualization of phagocytic activity of microglia (red: B, E, H). The merged images are shown in C, F, and I. Scale bar, 20 μm.

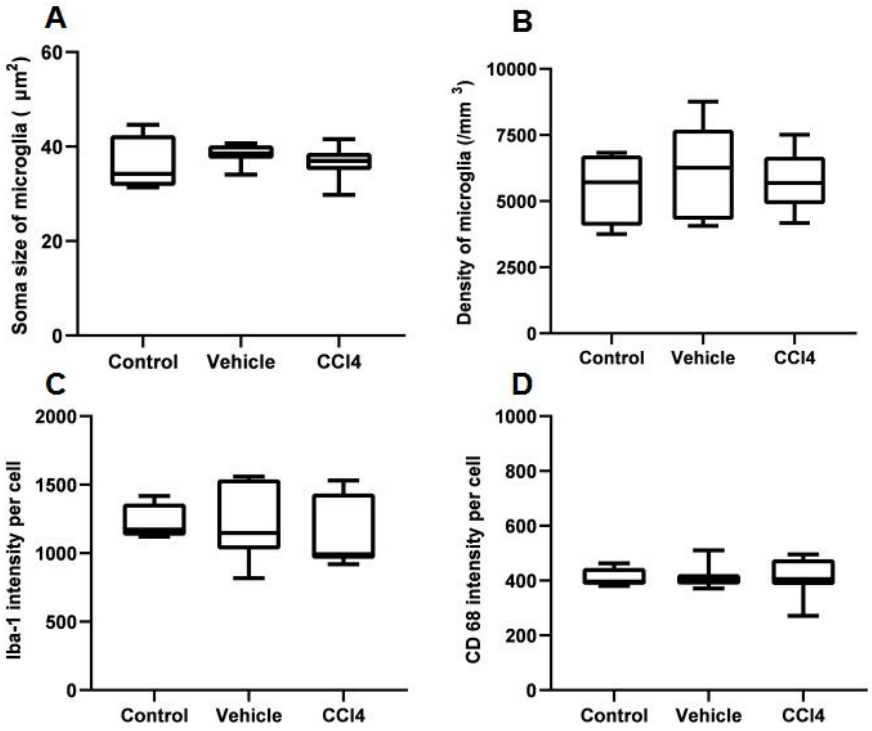

Figure 19. Severe liver fibrosis does not cause microglial activation in the VTA. Box-and-whisker plots showing the median (per mouse) soma size (A), density (B), Iba-1 (C) and CD 68 (D) fluorescence intensity of microglia in mice injected i.p. with 0.9% NaCl (Control, n = 4 mice), oil (Vehicle, n = 7 mice), or CCl4 (n = 7 mice) dissolved in oil (0.4 µl/g) two times per week over 9 weeks. There was no significant difference in the soma size, density, the Iba-1 and CD 68 fluorescence intensity of microglia in the VTA ($p > 0.05$ for all comparisons; Kruskal-Wallis test followed by post-hoc Dunn's correction, n = 4-7 mice per group, 5 areas per mouse).

There was no apparent morphological change of microglia in the VTA of mice with severe fibrosis (Fig. 18). Consistently, box-and-whisker plots also suggested there was no significant difference in the median (per mouse) soma size, density, the Iba-1 and CD 68 fluorescence intensity of microglia in the VTA (Fig. 19; $p > 0.05$ for all comparisons; Kruskal-Wallis test followed by post-hoc Dunn's correction, n = 4-7 mice per group, 5 areas per mouse).

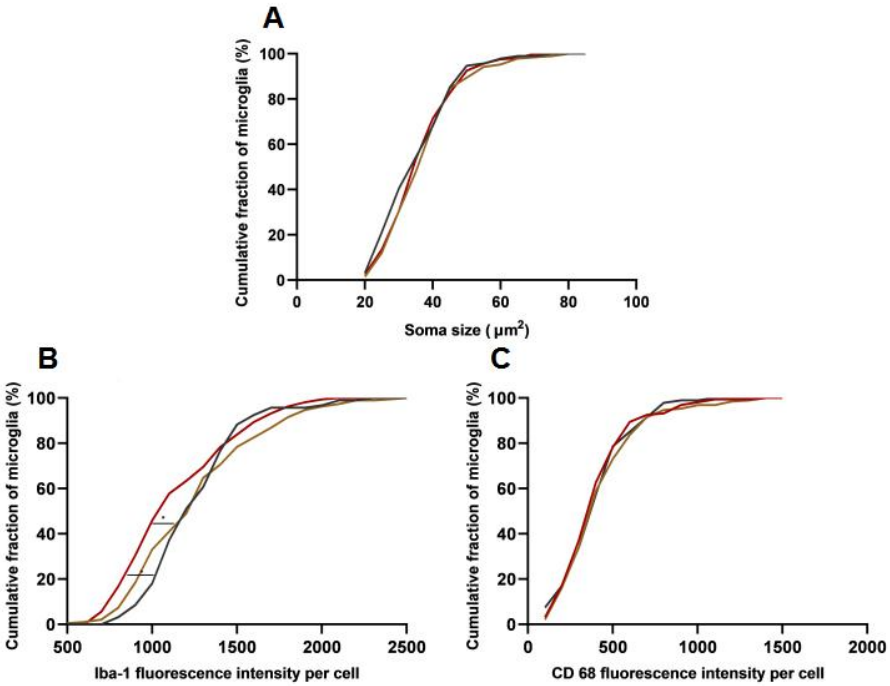

Figure 20. Mild changes of microglial soma size, as well as Iba-1 and CD 68 fluorescence in the VTA. Cumulative probability functions illustrating the distributions (per cell) of soma size (A) as well as Iba-1 (B) and CD 68 (C) fluorescence intensity in the SNr of mice injected i.p. with 0.9% NaCl (Control, black curve), oil (Vehicle, yellow curve), or CCl4 (red curve) dissolved in oil (0.4 µl/g) two times per week over 9 weeks (Control: n = 94 cells from 4 mice, Vehicle: n = 190 cells from 7 mice, CCl4: n = 161 cells from 7 mice). There was no significant difference in the distributions of soma size and CD 68 intensities in all comparisons ($p > 0.05$ for all comparisons, Kolmogorov-Smirnov test). The distribution of Iba-1 fluorescence intensity in mice treated with CCl4 was significantly shifted to the left when compared to the control and vehicle groups ($*p < 0.05$ for both comparisons, Kolmogorov-Smirnov test).

At the level of individual cells, there was no significant difference in the distributions of soma size and CD 68 fluorescence intensities in all comparisons (Fig. 20; $p > 0.05$ for all comparisons, Kolmogorov-Smirnov test). The distribution of Iba-1 fluorescence intensity in mice treated with CCl4 was significantly shifted to the left when compared to the control and vehicle groups ($*p < 0.05$ for both comparisons, Kolmogorov-Smirnov test). These data demonstrated that severe liver fibrosis is not accompanied by microglial activation in the VTA.

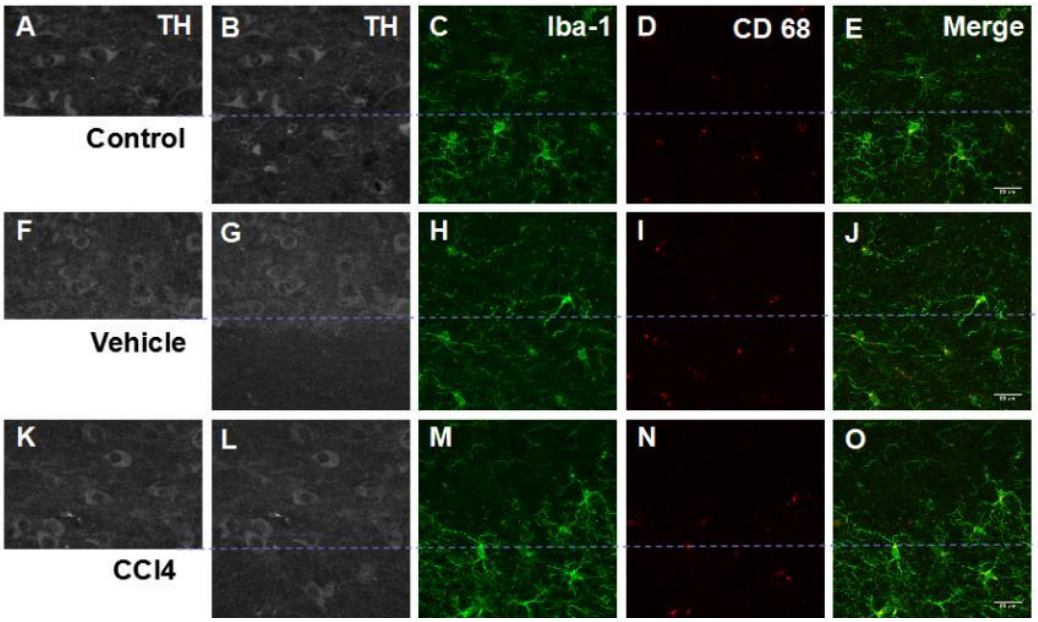

Figure 21. No apparent morphological change of microglia in the SNc of mice with severe fibrosis. MIP images (1-30 μm depth) of fixed brain slices of mice injected i.p. with 0.9% NaCl (Control), oil (Vehicle), or CCl4 dissolved in oil (0.4 μl/g) two times per week over 9 weeks. Coronal brain sections were stained with an anti-TH antibody for visualization of dopaminergic neurons (grey: A/B, F/G, K/L), an anti-Iba-1 antibody for visualization of microglia (green: C, H, M), and an anti-CD 68 antibody for visualization of phagocytic activity of microglia (red: D, I, N). The merged images are shown in E, J, and O. Scale bar, 20 μm.

Next, we studied the properties of microglia in the SN. We used the anti-TH labelling as a landmark, helping to find the border (a dotted line in Fig. 21) between SNc and SNr. As mentioned in the methods, we set the laser wavelength to 750 nm to capture the signal from TH^+ cells and then adjusted the position of the slices to ensure that the area rich in TH^+ cells (SNc) is located at the top of the images, and the area devoid of TH^+ cells (SNr) is located at the bottom. Note that SNc (i.e., the region located above the dotted line) has a lower density of microglia compared to SNr.

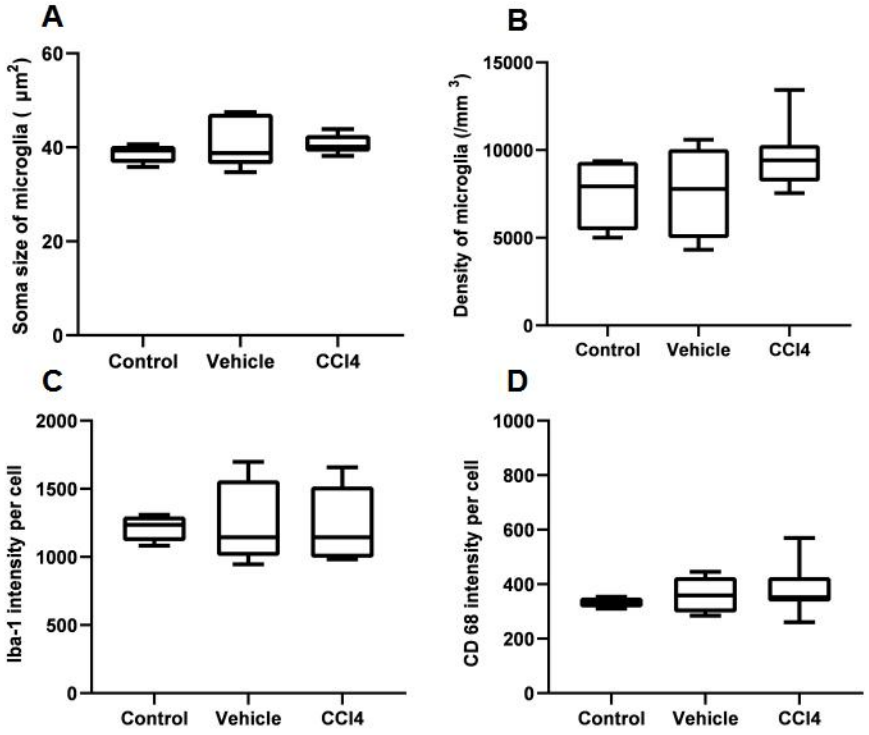

Figure 22. Severe liver fibrosis does not cause microglial activation in the SNc. Box-and-whisker plots showing the median (per mouse) soma size (A), density (B), Iba-1 (C) and CD 68 (D) fluorescence intensity of microglia in mice injected i.p. with 0.9% NaCl (Control, n = 4 mice), oil (Vehicle, n = 7 mice), or CCl4 (n = 7 mice) dissolved in oil (0.4 µl/g) two times per week over 9 weeks. There was no significant difference in the soma size, density, the Iba-1 and CD 68 fluorescence intensity of microglia in the SNc ($p > 0.05$ for all comparisons; Kruskal-Wallis test followed by post-hoc Dunn's correction, n = 4-7 mice per group, 5 areas per mouse).

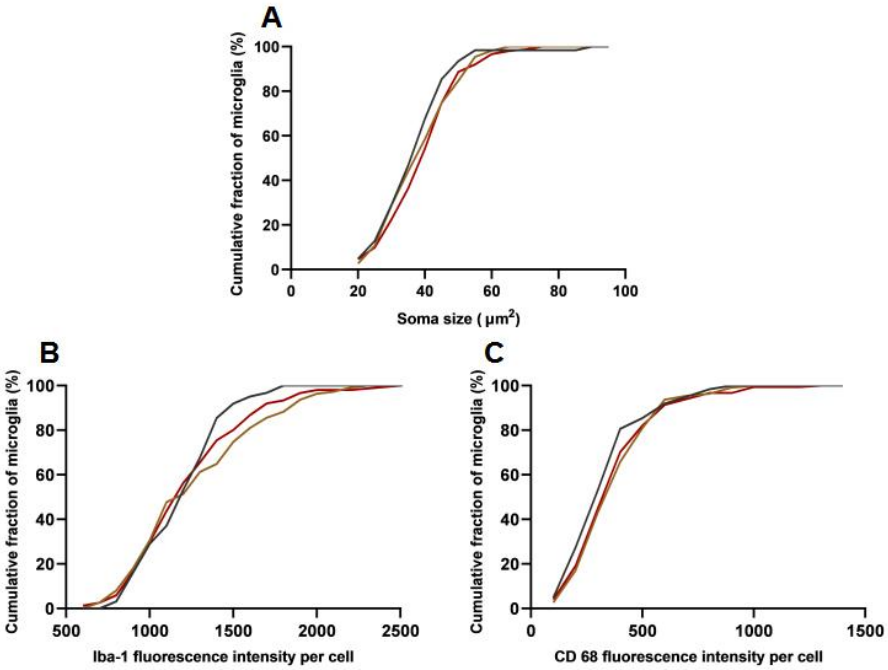

Figure 23. No changes of microglial soma size as well as Iba-1 and CD 68 fluorescence in the SNc. Cumulative

probability functions illustrating the distributions (per cell) of soma size (A) as well as Iba-1 (B) and CD 68 (C) fluorescence intensity in the SNr of mice injected i.p. with 0.9% NaCl (Control, black curve), oil (Vehicle, yellow curve), or CCl4 (red curve) dissolved in oil (0.4 µl/g) two times per week over 9 weeks (Control: n = 62 cells from 4 mice, Vehicle: n = 111 cells from 7 mice, CCl4: n = 151 cells from 7 mice). There was no significant difference in the distributions of soma size, density, the Iba-1, and CD 68 fluorescence intensity of microglia in all comparisons ($p > 0.05$ for all comparisons, Kolmogorov-Smirnov test).

There was no significant difference in the median (per mouse) soma size, density, the Iba-1 and CD 68 fluorescence intensity of microglia in the SNc ($p > 0.05$ for all comparisons; Kruskal-Wallis test followed by post-hoc Dunn's correction, n = 4-7 mice per group, 5 areas per mouse; Fig. 22), and these results were consistent with the data obtained at the single-cell level (Fig. 23).

Thus, the results obtained found no evidence for microglial activation in both SN (SNr and SNc) and VTA at the time point of 9 weeks. Thus, longer exposure to CCl4 did not cause stronger neuronal loss or microglial activation.

3.5. Severe liver fibrosis does not cause behavioural changes

To test whether the loss of dopaminergic neurons in the SNc is accompanied by motor deficits or anxiety, our cooperation partners in Hannover carried out two behavioural tests, including footprint analysis and open field test (OFT). The results were then analyzed in Tübingen. As shown in Fig. 24, footprint analysis did not reveal any significant difference in the fore-stride length, hind-stride length, fore-base width, hind-base width in comparisons between all the groups ($p > 0.05$ for all comparisons; Kruskal-Wallis test followed by post-hoc Dunn's correction, n = 4-9 mice per group).

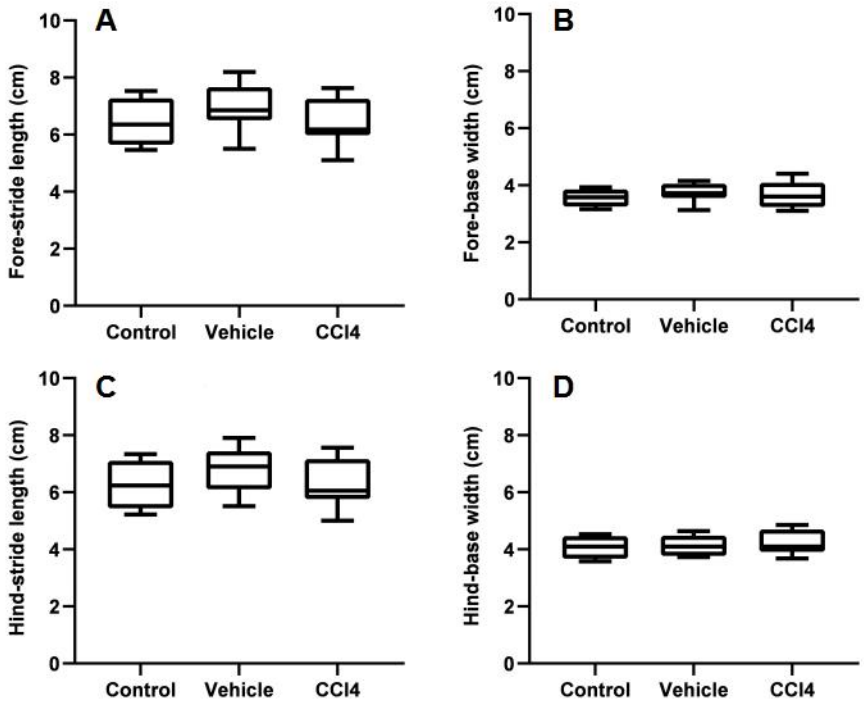

Figure 24. No changes of stride length and base width in mice with severe liver fibrosis. Box-and-whisker plots showing the median (per mouse) fore-stride length (A), fore-base width (B), hind-stride length (C) and hind-base width (D) in mice injected i.p. with 0.9% NaCl (Control, n = 4 mice), oil (Vehicle, n = 7 mice), or CCl4 (n = 9 mice) dissolved in oil (0.4 µl/g) two times per week over 9 weeks. The fore- or hind-stride length is the distance between the two consecutive travels of the same paw. The fore- or hind-base width is the distance between the right and the left forelimb or hindlimb stride. There was no significant difference in the fore-stride length, hind-stride length, fore-base width, hind-base width in all comparisons ($p > 0.05$ for all comparisons; Kruskal-Wallis test followed by post-hoc Dunn's correction, n = 4-9 mice per group).

For the OFT, no significant difference in the total distance, the distance in the central area and duration of movement in the central area in all comparisons were observed ($p > 0.05$ for all comparisons; Kruskal-Wallis test followed by post-hoc Dunn's correction, n = 3-8 mice per group; Fig. 25). These data suggest that there was no behavioural change in mice with severe liver fibrosis, at least, at the time point of 9 weeks.

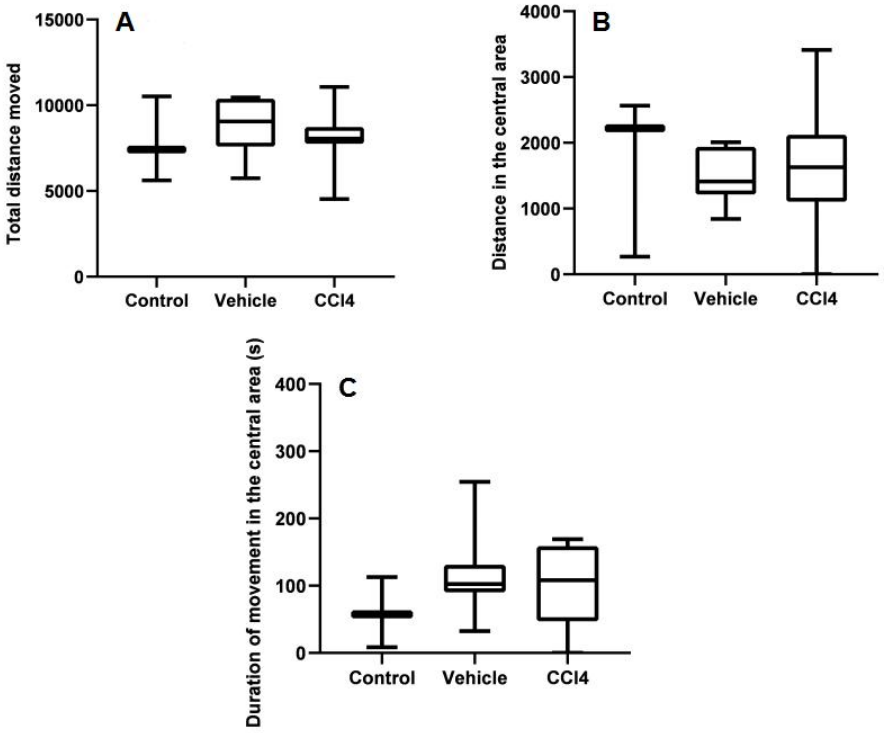

Figure 25. No changes of total distance, central area's distance and duration in the central area in mice with severe liver fibrosis. Box-and-whisker plots showing the median (per mouse) total distance (A), the distance in the central area (B) and duration of movement in the central area (C) in mice injected i.p. with 0.9% NaCl (Control, n = 3 mice), oil (Vehicle, n = 7 mice), or CCl4 (n = 8 mice) dissolved in oil (0.4 µl/g) two times per week over 9 weeks. There was no significant difference in the total distance, the distance in the central area and duration of movement in the central area in comparisons between all groups ($p > 0.05$ for all comparisons; Kruskal-Wallis test followed by post-hoc Dunn's correction, n = 3-8 mice per group).

3.6. No apparent loss of neurons in the SNc and VTA, after a single dose of CCl4

Because we did not observe a microglial response to the obvious damage of neurons at later time points, we hypothesized that microglial activation might precede the death of neurons and that these cells might already recover their ramified state at the analyzed time points. To test this hypothesis, we used a single dose of CCl4 and performed immunohistochemistry 36 h after the injection.

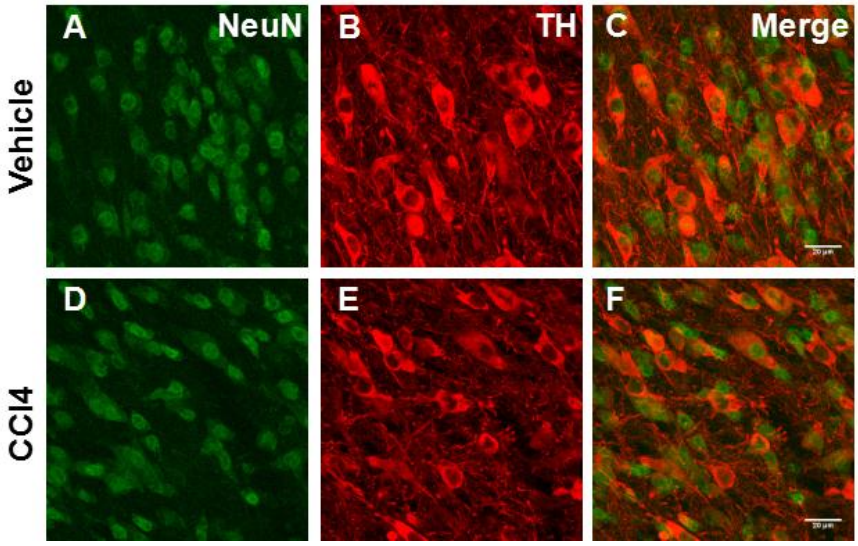

Figure 26. No apparent loss of neurons in the VTA of mice after a single dose of CCl4. MIP images (1-20 µm depth) of fixed brain slices of mice injected i.p. with oil (Vehicle), or CCl4 dissolved in oil (0.4 µl/g) 36 hours before the tissue fixation. Coronal brain sections were stained with an anti-NeuN antibody for visualization of neurons (green: A, D) and an anti-TH antibody for visualization of dopaminergic neurons (red: B, E). The merged images are shown in C, F. Scale bar, 20 µm.

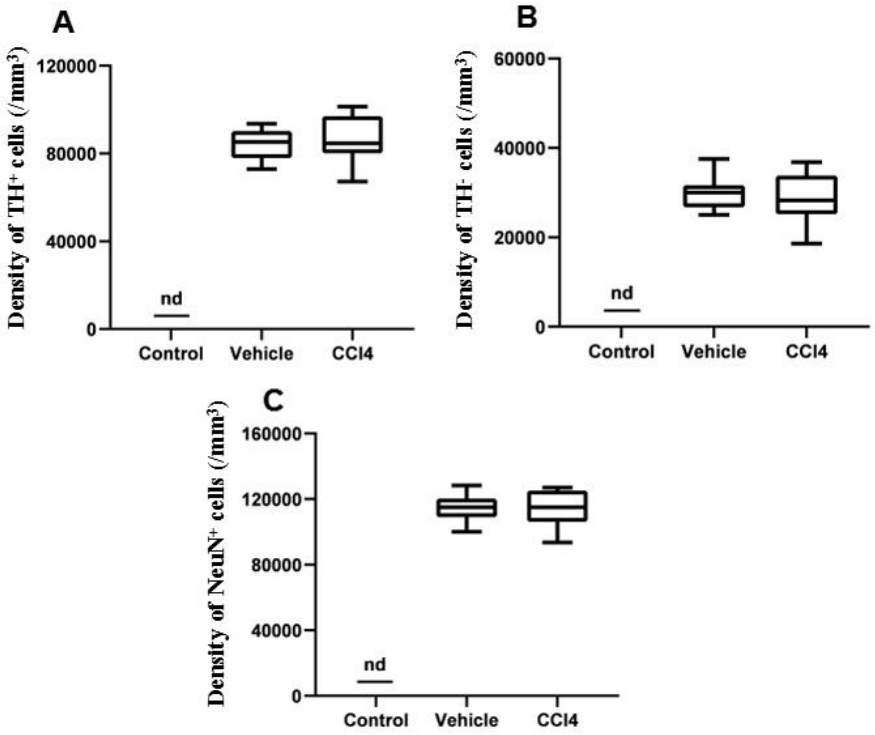

Figure 27. Exposure of mice to a single dose of CCl4 does not affect neuronal density in the VTA. Box-and-whisker plots showing the median (per mouse) density of TH^+ dopaminergic neurons (A), TH^- neurons (B) and any neurons (C) in mice injected i.p. with oil (Vehicle, n = 10 mice), or CCl4 (n = 10 mice) dissolved in oil (0.4

µl/g) a single time. There was no significant difference in the density of TH^+, TH^- or $NeuN^+$ neurons in the VTA ($p > 0.05$; Mann-Whitney test, n = 10 mice per group, 5 areas per mouse). nd, not detected.

There was no significant difference in the density of TH^+, TH^- or $NeuN^+$ neurons in the VTA (Fig. 26, 27) and SNc (Fig. 28, 29). Overall, these results indicate that CCl4-induced neurotoxicity does not cause a loss of neurons in the SNc and VTA at this early time point.

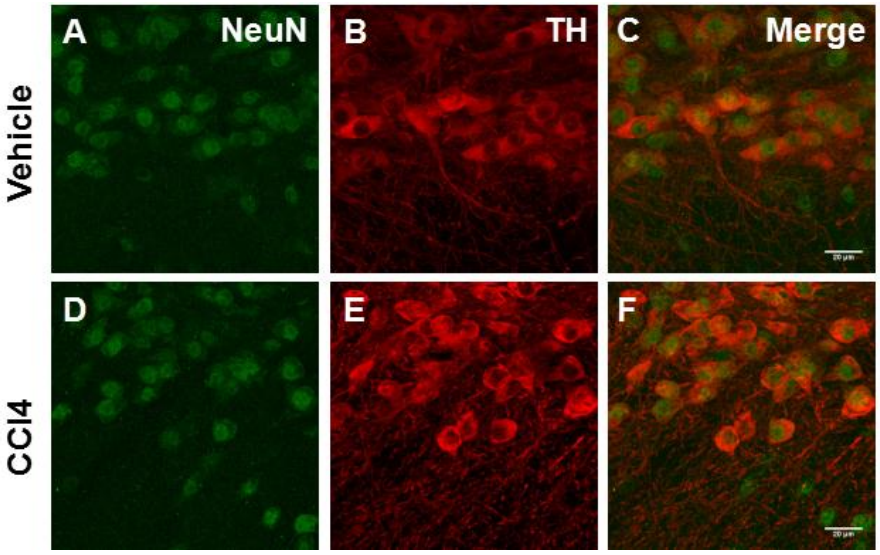

Figure 28. No apparent loss of neurons in the SNc of mice after a single dose of CCl4. MIP images (1-20 µm depth) of fixed brain slices of mice injected i.p. with oil (Vehicle), or CCl4 dissolved in oil (0.4 µl/g) a single time. Coronal brain sections were stained with an anti-NeuN antibody for visualization of neurons (green: A, D) and an anti-TH antibody for visualization of dopaminergic neurons (red: B, E). The merged images are shown in C, F. Scale bar, 20 µm.

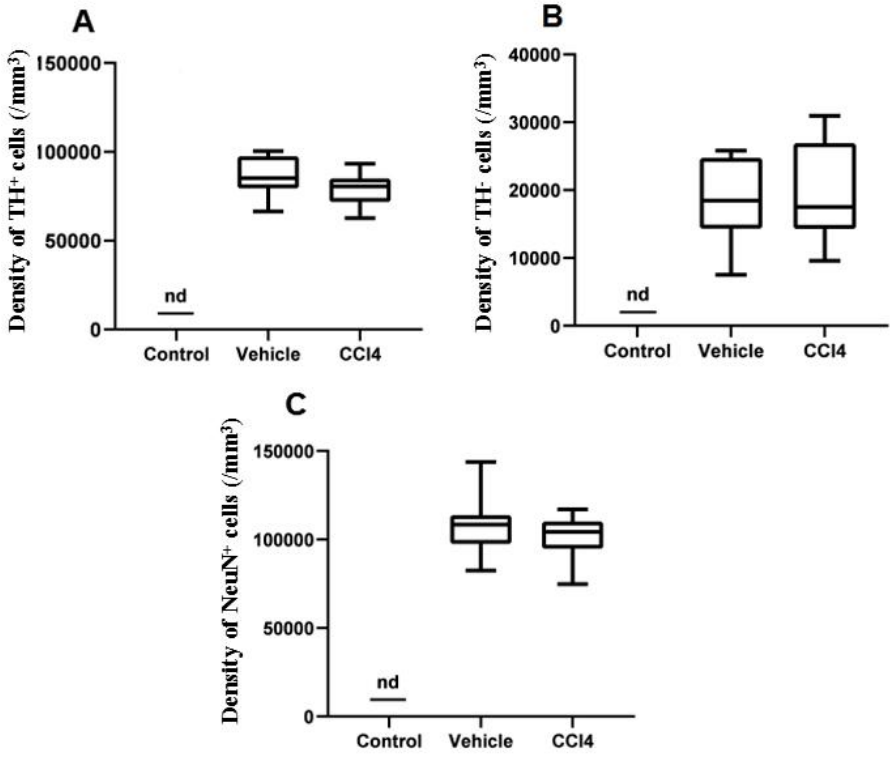

Figure 29. Exposure of mice to a single dose of CCl4 does not affect the neuronal density in the SNc. Box-and-whisker plots showing the median (per mouse) density of TH^+ dopaminergic neurons (A), TH^- neurons (B) and any neurons (C) in mice injected i.p. with oil (Vehicle, n = 10 mice), or CCl4 (n = 10 mice) dissolved in oil (0.4 µl/g) a single time. There was no significant difference in the density of TH^+, TH^- or $NeuN^+$ neurons in the SNc ($p > 0.05$; Mann-Whitney test, n = 10 mice per group, 5 areas per mouse). nd, not detected.

3.7. A single dose of CCl4 causes microglial activation characterized by increased soma size in the SNc and SNr

To further explore the changes in microglia within an acute period after CCl4 treatment, 20 mice were divided into 2 groups for statistical analysis. In the CCl4 group, there was a little bit of morphological change of microglia in the SNr of mice characterized by increased soma size. However, the microglia cell density and CD 68 fluorescence intensity seemingly did not change through direct observation (Fig. 30).

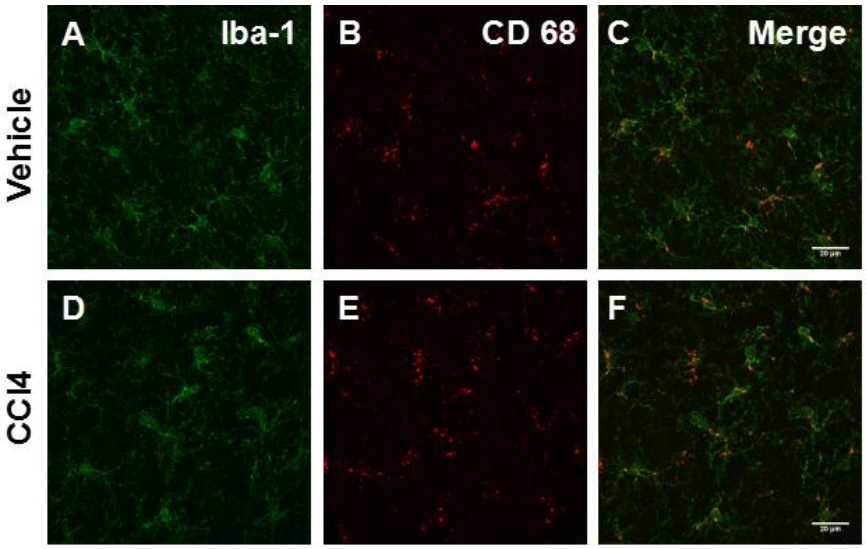

Figure 30. Apparent morphological change of microglia in the SNr of mice with a single dose CCl4. MIP images (1-30 µm depth) of fixed brain slices of mice injected i.p. with oil (Vehicle), or CCl4 dissolved in oil (0.4 µl/g) a single time, which were sacrificed 36 hours after treatment. Coronal brain sections were stained with an anti-Iba-1 antibody for visualization of microglia (green: A, D) and an anti-CD 68 antibody for visualization of phagocytic activity of microglia (red: B, E). The merged images are shown in C, F. Scale bar, 20 µm.

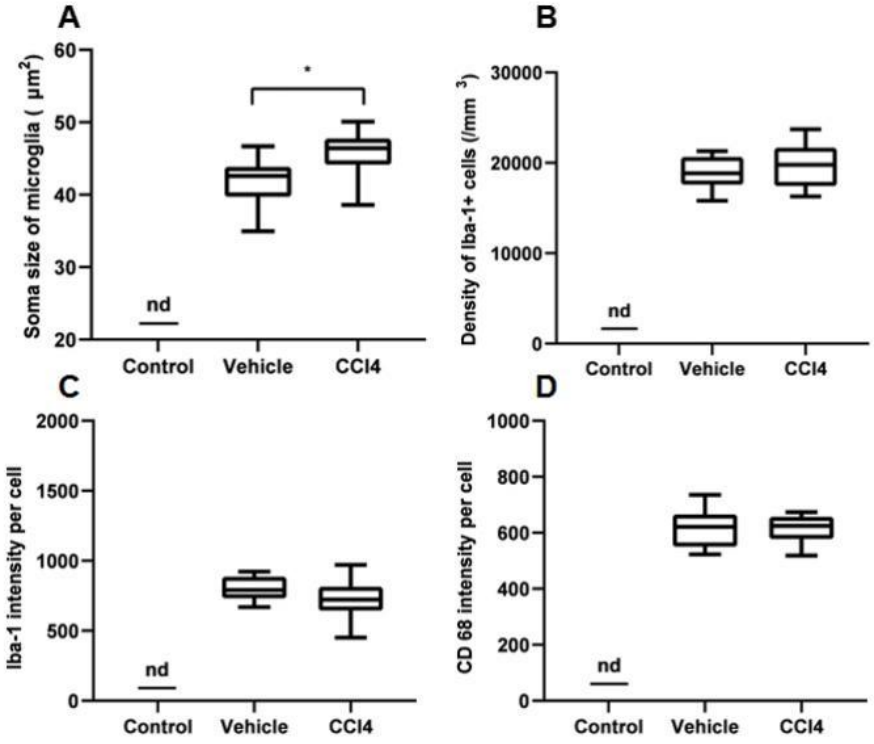

Figure 31. Exposure of mice to a single dose of CCl4 cause microglial activation in the SNr. Box-and-whisker plots showing the median (per mouse) soma size (A), density (B), Iba-1 (C) and CD 68 (D) fluorescence intensity of microglia in mice injected i.p. with oil (Vehicle, n = 10 mice), or CCl4 (n = 10 mice) dissolved in oil (0.4 µl/g) a single time. There was a significant difference in the soma size of microglia in the SNr (*p = 0.02; Mann-Whitney test, n = 10 mice per group, 5 areas per mouse). There was no significant difference in density, the Iba-1 and CD 68 fluorescence intensity of microglia in the SNr ($p > 0.05$ for all comparisons; Mann-Whitney test, n = 10 mice per

group, 5 areas per mouse). nd, not detected.

Interestingly, Comparing the oil and CCl4 groups, the median value of microglial cell soma size in the SNr increased from 42.58 to 46.43 μm^2, and there was a significant statistical difference (Fig. 31; *p = 0.02; Mann-Whitney test, n = 10 mice per group, 5 areas per mouse). Meanwhile, no significant difference in density, the Iba-1 and CD 68 fluorescence intensity of microglia in the SNr were detected (Fig. 31; p > 0.05 for all comparisons; Mann-Whitney test, n = 10 mice per group, 5 areas per mouse). These confirm that CCl4 can lead to an increase in the soma size of microglia in the SNr. However, the only drawback is that we lack the NaCl controls in the single-dose treatment group.

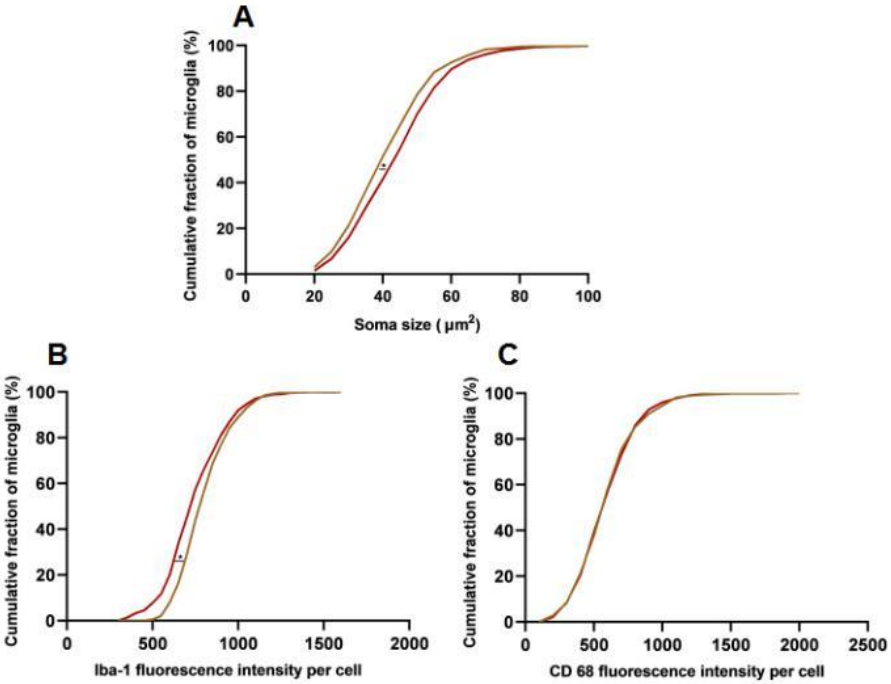

Figure 32. Moderate changes of microglial soma size and Iba-1 fluorescence, but not CD 68 fluorescence in the SNr. Cumulative probability function illustrating the distributions (per cell) of soma size (A) as well as Iba-1 (B) and CD 68 (C) fluorescence intensity in the SNr of mice injected i.p. with oil (Vehicle, yellow curve), or CCl4 (red curve) dissolved in oil (0.4 µl/g) a single time (Vehicle: n = 760 cells from 10 mice, CCl4: n = 800 cells from 10 mice). The distribution of soma size in mice treated with CCl4 was significantly shifted to the right when compared to the vehicle group (*p < 0.05, Kolmogorov-Smirnov test). The distribution of Iba-1 fluorescence intensity was shifted to the right in mice treated with oil when compared to the mice treated with CCl4 (*p < 0.05, Kolmogorov-Smirnov test). There was no difference in the distribution of CD 68 fluorescence intensity in the SNr (p > 0.05, Kolmogorov-Smirnov test).

At the level of individual cells, the distribution of soma size in mice treated with CCl4 was dramatically shifted to the right when compared to the vehicle group (Fig. 32; *p < 0.05, Kolmogorov-Smirnov test). The distribution of Iba-1 fluorescence intensity was shifted to the right in mice treated with oil when compared to the mice treated with CCl4 (Fig. 32; *p < 0.05, Kolmogorov-Smirnov test). There was no difference in the distribution of CD 68 fluorescence intensity in the SNr (Fig. 32; p > 0.05, Kolmogorov-Smirnov test).

Overall, the single most striking observation to emerge from the data comparison was that exposure to CCl4 can induce microglial activation in the SNr characterized by increased soma size. And CD 68, a marker for phagocytosis, is not changed, which also makes sense since there is nothing to phagocytose at this time point.

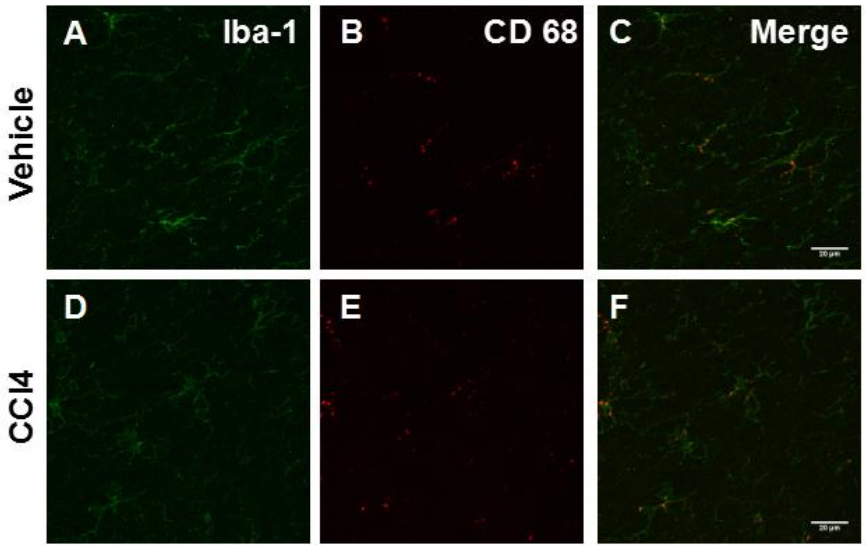

Figure 33. No apparent morphological change of microglia in the VTA of mice treated with a single-dose CCl4. MIP images (1-30 μm depth) of fixed brain slices of mice injected i.p. with oil (Vehicle), or CCl4 dissolved in oil (0.4 μl/g) a single time. Coronal brain sections were stained with an anti-Iba-1 antibody for visualization of microglia (green: A, D) and an anti-CD 68 antibody for visualization of phagocytic activity of microglia (red: B, E). The merged images are shown in C, F. Scale bar, 20 μm.

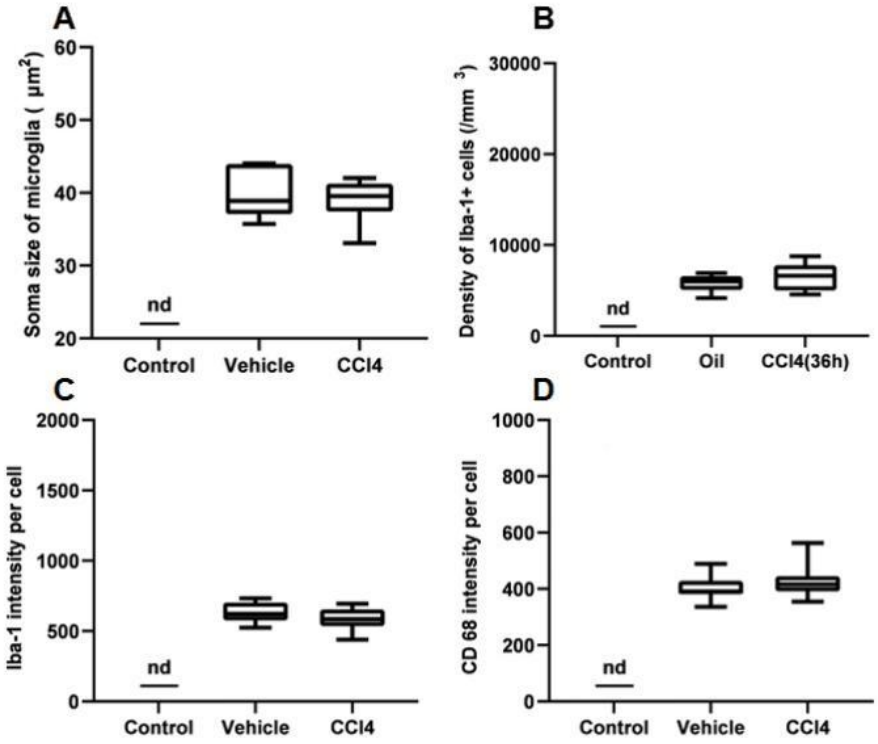

Figure 34. Exposure of mice to a single dose of CCl4 does not cause microglial activation in the VTA. Box-and-whisker plots showing the median (per mouse) soma size (A), density (B), Iba-1 (C) and CD 68 (D) fluorescence intensity of microglia in mice injected i.p. with oil (Vehicle, n = 10 mice), or CCl4 (n = 10 mice) dissolved in oil (0.4 µl/g) a single time. There was no significant difference in the soma size, density, the Iba-1 and CD 68 fluorescence intensity of microglia in the VTA ($p > 0.05$ for all comparisons; Mann-Whitney test, n = 10 mice per group, 5 areas per mouse). nd, not detected.

As mentioned above, to capture microglia in the SNc and VTA, we used an additional anti-TH antibody for visualization of dopaminergic neurons to locate the SNc and VTA. In Fig. 33, TH staining images used for positioning is not shown, there was no apparent morphological change of microglia in the VTA of mice treated with a single dose CCl4. The Box-and-whisker plots also suggested there was no significant difference in the median (per mouse) soma size, density, the Iba-1 and CD 68 fluorescence intensity of microglia in the VTA (Fig. 34; $p > 0.05$ for all comparisons; Mann-Whitney test, n = 10 mice per group, 5 areas per mouse).

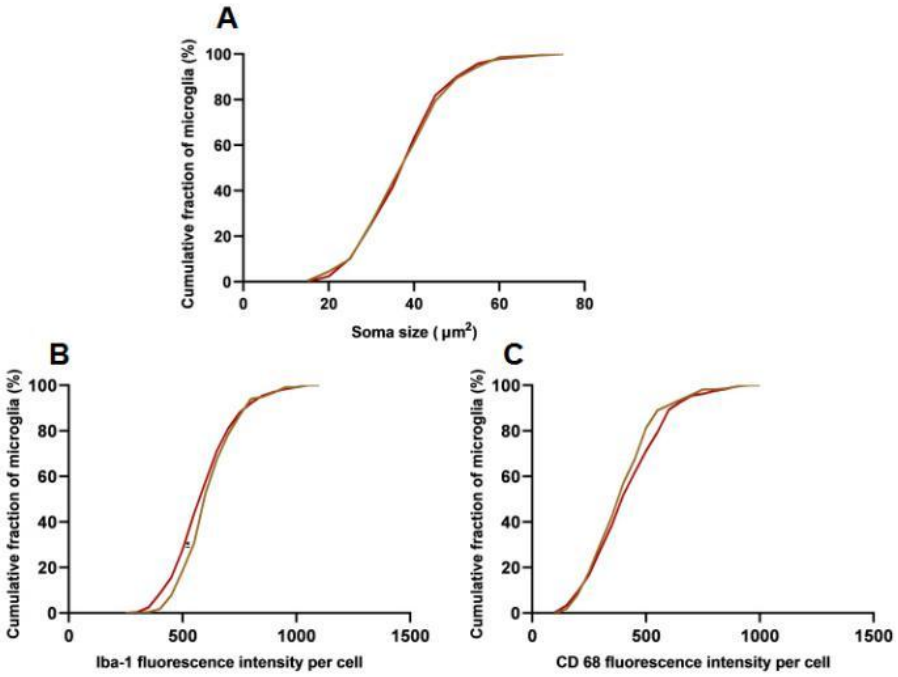

Figure 35. Mild changes of microglial soma size, as well as Iba-1 and CD 68 fluorescence in the VTA. Cumulative probability function illustrating the distributions (per cell) of soma size (A) as well as Iba-1 (B) and CD 68 (C) fluorescence intensity in the VTA of mice injected i.p. with oil (Vehicle, yellow curve), or CCl4 (red curve) dissolved in oil (0.4 μl/g) a single time (Vehicle: n = 219 cells from 10 mice, CCl4: n = 244 cells from 10 mice). There was no significant difference in the distributions of soma size and CD 68 fluorescence intensities in all comparisons ($p > 0.05$ for all comparisons, Kolmogorov-Smirnov test). The distribution of Iba-1 fluorescence intensity in mice treated with CCl4 was shifted to the left significantly when compared to the vehicle group (*$p < 0.05$, Kolmogorov-Smirnov test).

Similarly, there was no statistical difference in the distributions of soma size and CD 68 intensities for all comparisons (Fig. 35; $p > 0.05$ for all comparisons, Kolmogorov-Smirnov test). The distribution of Iba-1 fluorescence intensity in mice treated with CCl4 was shifted to the left significantly when compared to the vehicle group (Fig. 35; *$p < 0.05$, Kolmogorov-Smirnov test). In summary, these data demonstrated CCl4 does not cause microglial activation in the VTA.

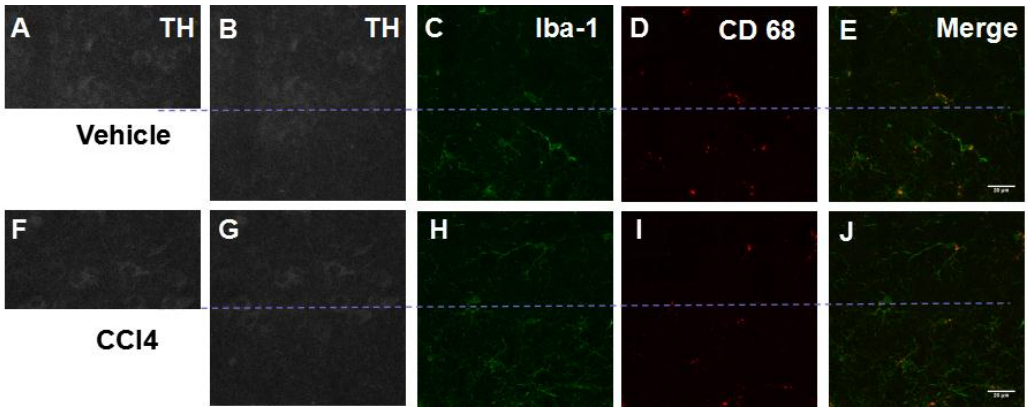

Figure 36. No apparent morphological change of microglia in the SNc of mice treated with a single dose of CCl4. MIP images (1-30 µm depth) of fixed brain slices of mice injected i.p. with oil (Vehicle), or CCl4 dissolved in oil (0.4 µl/g) a single time. Coronal brain sections were stained with an anti-TH antibody for visualization of dopaminergic neurons (grey: A/B, F/G), an anti-Iba-1 antibody for visualization of microglia (green: C, H) and an anti-CD 68 antibody for visualization of phagocytic activity of microglia (red: D, I). The merged images are shown in E, J. Scale bar, 20 µm.

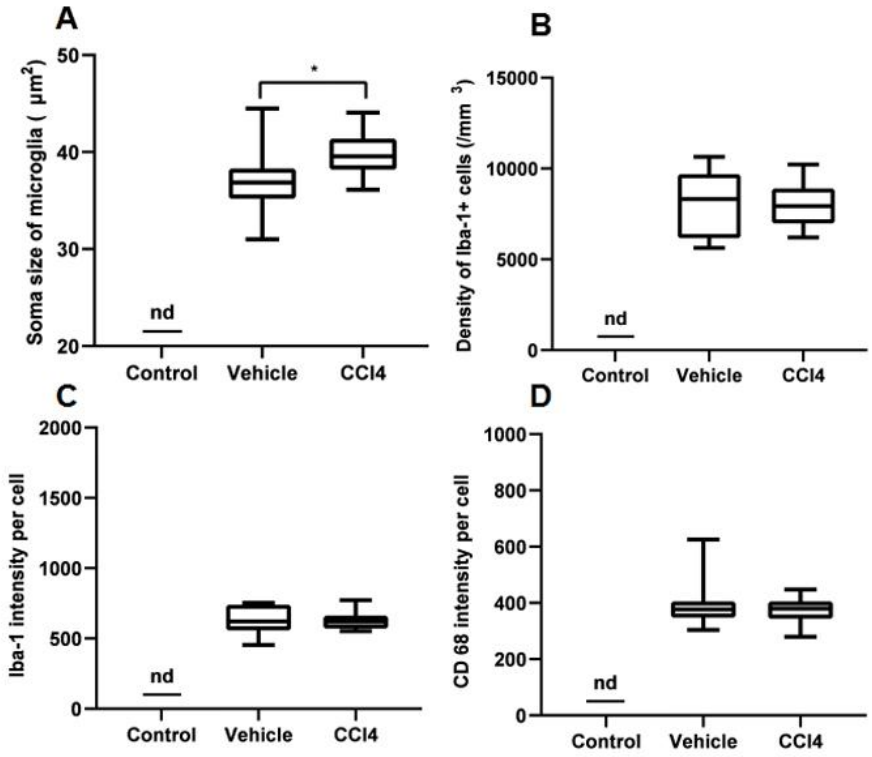

Figure 37. Exposure to single-dose CCl4 cause microglial activation in the SNc. Box-and-whisker plots showing the median (per mouse) soma size (A), density (B), Iba-1 (C) and CD 68 (D) fluorescence intensity of microglia in mice injected i.p. with oil (Vehicle, n = 10 mice), or CCl4 (n = 10 mice) dissolved in oil (0.4 µl/g) a single time. There was a significant difference in the soma size of microglia in the SNc (*p = 0.04; Mann-Whitney test, n = 10 mice per group, 5 areas per mouse). There was no significant difference in the density, the Iba-1 and CD 68 fluorescence intensity of microglia in the SNc ($p > 0.05$ for all comparisons; Mann-Whitney test, n = 10 mice per group, 5 areas per mouse). nd, not detected.

As shown in Fig. 36, the dotted line in the figure serves as the dividing line between SNc and SNr. SNc is the region above the dotted line, which has a lower density of microglia than SNr. Seemingly, there was no apparent morphological change of microglia in the SNc of mice injected with a single dose CCl4 (Fig. 36), but further analysis of the data reveals a significant increase in the soma size of microglia from 36.85 to 39.57 μm^2 in the SNc in CCl4 group compared with vehicle group (Fig. 37; *p < 0.05; Mann-Whitney test, n = 10 mice per group, 5 areas per mouse). For the distribution of soma size, the curve treated with CCl4 was shifted to the right when compared to that of the vehicle group (Fig. 38; p = 0.12; Vehicle: n = 152 cells from 10 mice, CCl4: n = 161 cells from 10 mice; Kolmogorov-Smirnov test). These data suggest that CCl4 can cause an increase in the soma size of microglia in the SNc at the early time point.

For the density, the Iba-1 and CD 68 fluorescence intensity of microglia in the SNc, Similar to the result in SNr and VTA, there was no significant difference between oil and CCl4 groups (Fig. 37; p > 0.05 for all comparisons; Mann-Whitney test, n = 10 mice per group, 5 areas per mouse), and the distribution result of Iba-1 and CD 68 fluorescence intensity was consistent with the analysis of previous Box-and-whisker plots (Fig. 38; p > 0. 5 for all comparisons; Vehicle: n = 152 cells from 10 mice, CCl4: n = 161 cells from 10 mice; Kolmogorov-Smirnov test). All of these suggest that the early response of a single-dose CCl4 can increase the soma size of microglia both in SNr and SNc.

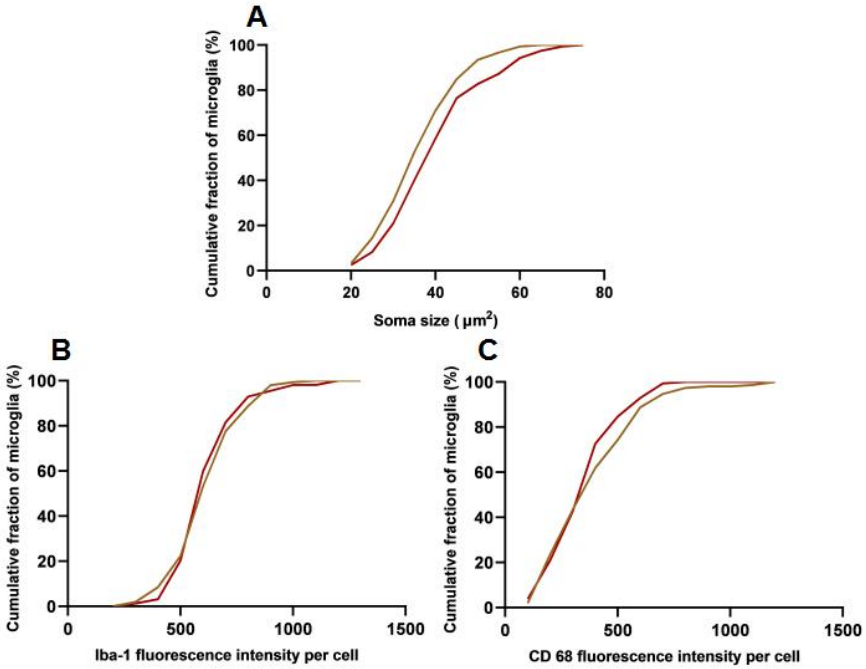

Figure 38. Moderate changes of microglial soma size, but not Iba-1 and CD 68 fluorescence in the SNc. Cumulative probability function illustrating the distributions (per cell) of soma size (A) as well as Iba-1 (B) and CD 68 (C) fluorescence intensity in the SNc of mice injected i.p. with oil (Vehicle, yellow curve), or CCl4 (red curve) dissolved in oil (0.4 µl/g) a single time (Vehicle: n = 152 cells from 10 mice, CCl4: n = 161 cells from 10 mice). The distribution of microglial soma size in mice treated with CCl4 was shifted to the right when compared to the vehicle group ($p = 0.12$, Kolmogorov-Smirnov test). There was no significant difference in the distribution of the Iba-1 and CD 68 fluorescence intensity of microglia in all comparisons ($p > 0.05$ for all comparisons, Kolmogorov-Smirnov test).

Taken together, all results described here indicated that microglia in the SNc, SNr and VTA did not show morphological alterations at the time point of the mild (4 weeks) and severe (9 weeks) liver fibrosis we investigated. However, the activated microglia characterized by increased soma size was established in both SNr and SNc at the early phase of the single-dose CCl4 treatment (36h). These findings remind us that the soma size of microglia in SN seems to have returned to normal status within few days, before 4 weeks. Hence, it seems difficult to explain the relationship between microglia and neuron loss. But, during 4 weeks and 9 weeks, the becoming stable microglia seems to be consistent with the stagnation in the progress of neuronal loss. Additionally, the unexpected outcome from the single-dose CCl4 group shows that a single injection of CCl4 can cause microglial activation characterized by increased soma size in the SNc

and SNr, but not in the VTA and this microglial activation precedes neuronal loss.

4. Discussion

A strong relationship between liver disease and Parkinsonism has been reported in the literature. In the present work, we used the CCl4-induced hepatic inflammation model over three time periods (4 weeks, 9 weeks, 36 hours), and observed changes in neurons and microglia in the midbrain tissue using immunohistochemistry and 2-photon microscopy. Our data show that (i) CCl4-induced neurotoxicity moderately but significantly cause a loss of dopaminergic neurons in the SNc, but not in the VTA. (ii) Longer exposure to CCl4 did not further cause more neurons to be lost, or microglia activation. (iii) The early response to single-dose CCl4 can increase the soma size of microglia both in SNr and SNc. (iv) The oil itself can induce a slight activation of microglia in the SNr.

It is believed that neurons in the SN are more susceptible than those in the VTA, and the mechanism is still unknown. Some scholars have suggested that this difference is mainly related to the balance of glial cells, astrocytes that provide protective factors and microglia that release deleterious cytokines (Ji et al. 2016, Smeyne et al. 2001). Indeed, to investigate the susceptibility of neurons, Eric and colleagues isolated astrocytes, microglia and dopaminergic neurons from the SN and VTA in rats. The neurotoxic drug, 1-methyl-4-phenylpyridium (MPP^+), was used in their vitro experiment. They found that both SN and VTA isolated microglia can be activated by MPP^+ and exacerbated MPP^+ neurotoxic effects. Interestingly, they showed that astrocytes, derived from VTA rather than SN, were capable to protect dopaminergic neurons in SN and VTA, even in the presence of harmful microglia. However, this protection can be reversed by increasing the number of microglia (Wildon et al. 2018). Thus, the different distribution and balance of microglia and astrocytes may be the key factor that causes the different susceptibility between SN and VTA (Damier et al. 1993, Wildon et al. 2018).

Our results indicate that the density of neurons in the VTA of mice treated with CCl4 i.p. did not change at any time point, the microglia in morphology, density, Iba-1

and CD 68 protein expression remained unchanged. However, under the same conditions, a significant reduction of dopaminergic neurons in the SNc was observed in the 4 and 9- weeks CCl4-treated groups, while the number of neurons did not change in the 36-hour treatment group. On the other hand, we found that microglia in the SNc and SNr became larger in soma size after early CCl4-treatment, but this phenomenon was not detected in the 4 and 9- week treatment groups, this suggests that the soma size of microglia gradually returns to normal status possibly in 4 weeks. These results imply that both dopaminergic neurons and microglia in SN are more vulnerable than VTA in C57BL/6J mice treated with CCl4.

Our data suggest that neuronal loss in the SNc occurs in mice with mild fibrosis. Here, approximately 40% of neurons are lost. Surprisingly, this effect is not aggravated in mice with severe fibrosis, in which neuronal loss amounted to approximately 30%. These reveal that any sustained or aggravated liver damage, neurotoxins, oxidative stress, or even potential blood ammonia increase induced by CCl4 did not result in further neuronal loss during 4 - 9 weeks. This tendency of neurons to stop losing seems to be highly consistent with the continuous resting state of microglia. Therefore, our results suggest that the severity of CCl4-induced cirrhosis does not aggravate neuronal loss in the short term. However, for patients with hepatic encephalopathy caused by long-term cirrhosis, microglial activation and neuron loss may still occur due to multiple factors such as oxidative stress, neuroinflammation, and hyperammonemia (Victoria et al. 2017). So, if we continue to observe cirrhotic mice for a few months or longer, we may discover a further neuronal loss in SNc.

What is the relationship between dopaminergic neuronal loss and activated microglia in SN of mice treated with CCl4? It is generally believed that microglial activation precedes neuronal loss and neurons undergoing degeneration may be devoured prematurely by phagocytic microglia (Lull and Block 2010, Marinova-Mutafchieva et al. 2010, Sung et al. 2012). We hypothesize that CCl4 causes microglial activation, which further leads to neuronal loss. To confirm our conjecture,

we observed changes in neurons and microglia 36 hours after a single intraperitoneal injection of CCl4 in mice, what is surprising is that no neuronal loss was found, but soma size of microglia was increased in the SNc and SNr. There are two possibilities for these results, that CCl4 directly induces microglial activation preceding neuronal loss or neurons are already affected, but not yet dead, they could signal their dysfunctional state to microglia (e.g. by altered activity or altered fractalkine signalling or others), which then start to activate.

Interestingly, no microglia activation was detected in either the 4 weeks or 9 weeks CCl4-treated mice. In addition to the microglia becoming resting, another possibility is related to the age of the mice we used. Sugama and colleagues found that neurons are more likely to be lost in the SN of older (9- 12 months old) mice and that microglia are more prone to be activated than young mice (3 months old) (Sugama et al. 2003). Indeed, age-dependent microglia activation has been reported in aged rodents (Perry et al. 2010a), rats (Ogura et al. 1994), humans (Streit and Sparks 1997), and other primates (Sheffield and Berman 1998), whereas the specific mechanism of age-related microglial activation remains unknown. Even then, it is unclear whether it is the ageing microglia that causes the increase in neurodegeneration in the elderly, or the ageing neurons themselves are more susceptible to degenerative cues (Spittau 2017).

CCl4 can induce peripheral systemic inflammation, which is thought to insult the CNS through multiple pathways (Block and Calderón-Garcidue?As 2009, Erickson et al. 2012). Of particular note is that peripheral inflammation can activate NF-κB signalling, which produces downstream pro-inflammatory mediators such as TNF-α, IL-1, IL-6, and many others (Chen et al. 2015, Wang et al. 2009). There is evidence that the serum TNF-α level is significantly increased at 24 hours after a single intraperitoneal injection of CCl4 (Han et al. 2017, Kim et al. 2011). TNF-α has been confirmed to enter the brain through a relatively permeable region of the BBB, the circumventricular organ, and induce microglial and astrocytic activation, causing neuroinflammation. Additionally, IL-1β and IL-6 are also thought to play a vital role in causing neuroinflammation via a

liver-brain axis (D'Mello et al. 2011). These studies identified that chronic exposure to elevated inflammatory cytokines can trigger an inflammatory response in the CNS that causes impairments in neurons. In our present study, CCl4 induced cirrhotic mice occurred loss of nearly 30- 40% of dopaminergic neurons in the SNc. However, we did not detect any symptoms of Parkinsonism through the analysis of footprint and OFT. The reason may be that, the loss rate of dopaminergic neurons in our animal model is less than 50%. On the other hand, this experiment lacks the detection of dopamine concentration and the condition of DR in the striatum. Therefore, it is necessary to detect the behaviour of mice with cirrhosis induced by CCl4 for a longer time.

5. Limitation

Present work lacks the detection of astrocytes. After all, astrocytes are also considered to work with microglia to determine the susceptibility of the SN (Wildon et al. 2018). From the research of primary cultured neurons and astrocytes separated from the chick embryo brain exposed to CCl4, it was confirmed that the metabolic activation of CCl4 in neurons was higher than that of astrocytes, and astrocytes appear to have a stronger anti-toxic effect than neurons (Clemedson et al. 1990, Clemedson et al. 1994).

6. Summary

There is growing evidence showing that chronic liver diseases, often accompanied by liver inflammation and fibrosis, are not limited to the liver, but comprise several organs, especially the brain. Moreover, recent epidemiological studies revealed a strong relationship between Parkinsonism and several liver diseases. In the present work, we used a liver inflammation model, induced by carbon tetrachloride (CCl4). CCl4 is metabolized by the hepatocytes to form the toxic trichloromethyl radical (CCl•3), which disrupts the lipid metabolism in the liver. In this hepatic inflammation model, we analyzed the pathological changes in midbrain neurons and microglia using immunohistochemistry and 2-photon microscopy. CCl4 was given over three different periods (36 hours, 4, and 9 weeks) to mimic both the acute and the chronic phases of inflammation. The data revealed surprisingly early (36 hours after the first CCl4 injection) signs of microglial activation in both SNr and SNc but not in the VTA and moderate but significant and selective loss of dopaminergic neurons in the SNc after both 4- and 9-week-long CCl4 treatments. The latter, however, was not accompanied by abnormalities in motor behaviour.

Together, these findings suggest that microglia, activated right at the beginning of liver-mediated inflammation, might trigger/cause the loss of dopaminergic neurons in SNc. The parkinsonian symptoms might be the consequence.

7. Zusammenfassung

Es gibt immer mehr Hinweise darauf, dass chronische Lebererkrankungen, die oft mit Leberentzündung und Fibrose einhergehen, nicht auf die Leber beschränkt sind, sondern mehrere Organe, insbesondere das Gehirn, umfassen. Darüber hinaus haben neuere epidemiologische Studien einen starken Zusammenhang zwischen Parkinsonismus und verschiedenen Lebererkrankungen beschrieben. In der vorliegenden Arbeit haben wir ein Leberentzündungsmodell verwendet, das durch Tetrachlorkohlenstoff (CCl4) induziert wurde. CCl4 wird von den Hepatozyten zu dem toxischen Trichlormethylradikal (CCl•3) verstoffwechselt, das den Lipidstoffwechsel in der Leber stört. In diesem Leberentzündungsmodell analysierten wir die pathologischen Veränderungen in Neuronen und Mikroglia des Mittelhirns mittels Immunhistochemie und Zwei-Photonen Mikroskopie. CCl4 wurde über drei verschiedene Zeiträume (36 Stunden, 4 und 9 Wochen) verabreicht, um sowohl die akute als auch die chronische Phase der Entzündung zu imitieren. Die Daten zeigten überraschend frühe (36 Stunden nach der ersten CCl4-Injektion) Anzeichen einer mikroglialen Aktivierung sowohl im SNr als auch im SNc, aber nicht im VTA; und einen moderaten, aber signifikanten und selektiven Verlust dopaminerger Neuronen im SNc sowohl nach 4- als auch 9-wöchiger CCl4-Behandlung. Letzteres war jedoch nicht von der Beeinträchtigung des motorischen Verhaltens begleitet.

Zusammenfassend, deuten diese Befunde darauf hin, dass Mikroglia, die gleich zu Beginn der Leber-vermittelten Entzündung aktiviert werden, den Verlust dopaminerger Neuronen im SNc auslösen/verursachen könnten. Die parkinsonschen Symptome könnten die Folge sein.

8. References

Beier E, Neal M, Alam G, Edler M, Wu LJ and Richardson JR (2017) Alternative microglial activation is associated with cessation of progressive dopamine neuron loss in mice systemically administered lipopolysaccharide. *Neurobiology of Disease*: S0969996117301821.

Block ML and Calderón-Garcidue?As L (2009) Air pollution: mechanisms of neuroinflammation and CNS disease. *Trends in Neurosciences 32*: 506-516.

Burkhard PR, Delavelle J, Du PR and Spahr L (2003) Chronic Parkinsonism Associated With Cirrhosis: A Distinct Subset of Acquired Hepatocerebral Degeneration. *Archives of Neurology 60*: 521.

Butterworth and Roger F (2013a) The liver-brain axis in liver failure: neuroinflammation and encephalopathy. *Nature Reviews Gastroenterology & Hepatology 10*: 522-528.

Butterworth and Roger F (2013b) Parkinsonism in cirrhosis: pathogenesis and current therapeutic options. *Metabolic Brain Disease 28*: 261-267.

Butterworth RF (2011) Hepatic encephalopathy: a central neuroinflammatory disorder? *Hepatology 53*: 1372-1376.

Butterworth RF, Spahr L, Fontaine S and Layrargues GP (1996) Manganese toxicity, dopaminergic dysfunction and hepatic encephalopathy. *Metabolic Brain Disease 10*: 259-267.

Chen L, Deng H, Cui H, Fang J and Ling Z (2015) Inflammatory responses and inflammation-associated diseases in organs. *Oncotarget 9*: 7204-7218.

Claudia, D., Umphlet, Ariana, Quattlebaum, Kaela, R. S and Reinert (2014) Short-term effects of an endotoxin on substantia nigra dopamine neurons. *Brain research 1557*: 164-170.

Clemedson C, Odland L and Walum E (1990) Differential effect of carbon tetrachloride on the cell membranes of neurons and astrocytes. *Neurotoxicology and Teratology 12*: 597-602.

Clemedson C, Romert L, Odland L, Varnbo I and Walum E (1994) Biotransformation of carbon tetrachloride in cultured neurons and astrocytes. *Toxicology in Vitro An International Journal Published in Association with Bibra 8*: 145-152.

Cousins DA, Butts K and Young AH (2010) The role of dopamine in bipolar disorder. *Bipolar Disorders 11*: 787-806.

D'Mello C and Swain MG (2011) Liver-brain inflammation axis. *American Journal of Physiology Gastrointestinal & Liver Physiology 301*: G749.

D'Mello C and Swain MG, *Immune-to-Brain Communication Pathways in Inflammation-Associated Sickness and Depression*. Inflammation-Associated Depression: Evidence, Mechanisms and Implications: 2016.

Damier P, Hirsch E, Zhang P, Agid Y and Javoy-Agid F (1993) Glutathione peroxidase, glial cells and Parkinson's disease. *Neuroscience 52*: 1-6.

Erickson MA, Dohi K and Banks WA (2012) Neuroinflammation: A Common Pathway in CNS Diseases as Mediated at the Blood-Brain Barrier. *NeuroImmunoModulation 19*: 121-130.

Eriksen N, Stark AK and Pakkenberg B (2009) Age and Parkinson's Disease-Related Neuronal Death in the Substantia Nigra Pars Compacta. *Journal of Neural Transmission Supplementum*.

Garcia-Martinez R and Cordo Ba J (2012) Liver-induced inflammation hurts the brain. *Journal of Hepatology 56*: 515-517.

Gayle DA, Ling ZD, Tong CW, Landers T and Carvey PM (2002) Lipopolysaccharide (LPS)-induced dopamine cell loss in culture: roles of tumor necrosis factor-alpha, interleukin-1beta, and nitric oxide.

Developmental Brain Research 133: 27-35.

Goehler LE, Gaykema R, Hansen MK, Anderson K and Watkins LR (2000) Vagal immune-to-brain communication: a visceral chemosensory pathway. *Autonomic Neuroscience Basic & Clinical 85*: 49-59.

Han J, Wang D, Li D, Chen X, Wang B, Wang F, Liu X, Shang J and Zheng Q (2017) Licochalcone E protects against carbon tetrachloride-induced liver toxicity by activating peroxisome proliferator-activated receptor gamma. *Molecular Medicine Reports*.

Henry CJ, Yan H, Wynne A, Hanke M, Himler J, Bailey MT, Sheridan JF and Godbout JP (2008) Minocycline attenuates lipopolysaccharide (LPS)-induced neuroinflammation, sickness behavior, and anhedonia. *Journal of Neuroinflammation,5,1(2008-05-13) 5*: 15-15.

Henry CJ, Yan H, Wynne AM and Godbout JP (2009) Peripheral lipopolysaccharide (LPS) challenge promotes microglial hyperactivity in aged mice that is associated with exaggerated induction of both pro-inflammatory IL-1β and anti-inflammatory IL-10 cytokines. *Brain Behavior & Immunity 23*: 309-317.

Ji Z, Yang B, Sun H, Yan Z and Gang H (2016) Aquaporin-4 deficiency diminishes the differential degeneration of midbrain dopaminergic neurons in experimental Parkinson's disease. *Neuroscience Letters 614*: 7-15.

Kim HY, Park J, Lee KH, Lee DU and Lee SM (2011) Ferulic acid protects against carbon tetrachloride-induced liver injury in mice. *Toxicology 282*: 104-111.

Kim JM, Ji SK, Jeong SH, Yu KK, Sang EK, Kim SH and Kim Y (2010) Dopaminergic neuronal integrity in parkinsonism associated with liver cirrhosis. *Neurotoxicology 31*: 351-355.

Levy, Barry S, Nassetta and William J (2003) Neurologic Effects of Manganese in Humans: A Review. *International Journal of Occupational and Environmental Health*.

Liedtke C, Luedde T, Sauerbruch T, Scholten D, Streetz K, Tacke F, Tolba R, Trautwein C, Trebicka J and Weiskirchen R (2013) Experimental liver fibrosis research: update on animal models, legal issues and translational aspects. *Fibrogenesis Tissue Repair 6*.

Ling EA and Wong WC (2010) The origin and nature of ramified and amoeboid microglia: a historical review and current concepts. *Glia 7*: 9–18.

Lull ME and Block ML (2010) Microglial Activation and Chronic Neurodegeneration. *Journal of the American Society for Experimental NeuroTherapeutics 7*: 354-365.

Marinova-Mutafchieva L, Sadeghian M, Broom L, Davis JB, Medhurst AD and Dexter DT (2010) Relationship between microglial activation and dopaminergic neuronal loss in the substantia nigra: a time course study in a 6‐hydroxydopamine model of Parkinson's disease. *Journal of Neurochemistry 110*: 966-975.

Mcdonald C, Newton J, Lai HM, Baker SN and Jones DE (2010) Central nervous system dysfunction in primary biliary cirrhosis and its relationship to symptoms. *Journal of Hepatology 53*: 1095-1100.

Meck WH (2006) Neuroanatomical localization of an internal clock: A functional link between mesolimbic, nigrostriatal, and mesocortical dopaminergic systems. *Brain Research 1109*: 93-107.

Mhyre T, Boyd J and Hamill R (2012) Parkinson's Disease. *Sub-cellular biochemistry 65*: 389.

Morris GP, Clark IA, Zinn R and Vissel B (2013) Microglia: A new frontier for synaptic plasticity, learning and memory, and neurodegenerative disease research. *Neurobiology of Learning and Memory 105*.

Ogura KI, Ogawa M and Yoshida M (1994) Effects of ageing on microglia in the normal rat brain:

immunohistochemical observations. *Neuroreport 5*: 1224.

Paquet KJ and Kamphausen U (1975) The carbon-tetrachloride-hepatotoxicity as a model of liver damage. First report: Long-time biochemical changes. *Acta hepato-gastroenterologica 22*: 84.

Perl DP and Warren OC (2007) The Neuropathology of Manganese-Induced Parkinsonism. *Journal of Neuropathology & Experimental Neurology*: 675-682.

Perry VH, Matyszak MK and Fearn S (2010a) Altered antigen expression of microglia in the aged rodent CNS. *Glia 7*: 60–67.

Perry VH, Nicoll J and Holmes C (2010b) Microglia in neurodegenerative disease. *Nature Reviews Neurology 6*: 193.

Perry VH and Teeling J (2013) Microglia and macrophages of the central nervous system: the contribution of microglia priming and systemic inflammation to chronic neurodegeneration. *Seminars in Immunopathology 35*: 601-612.

Qin L, Li G, Qian X, Liu Y and Block ML (2010) Interactive role of the toll-like receptor 4 and reactive oxygen species in LPS-induced microglia activation. *Glia 52*: 78-84.

Ransohoff RM and Perry VH (2009) Microglial Physiology: Unique Stimuli, Specialized Responses. *Annual Review of Immunology 27*: 119-145.

Rocha S, Fran?A M, Rodrigues GB, Barbosa K, Nunes A, Pastor AF, Oliveira A, Oliveira WH, Luna R and Peixoto CA (2014) Diethylcarbamazine Reduces Chronic Inflammation and Fibrosis in Carbon Tetrachloride- (CCl4-) Induced Liver Injury in Mice. *Mediators of Inflammation 2014*: 696383.

Santoro A, Mancini E, Ferramosca E and Faenza S (2007) Liver support systems. *Contributions to Nephrology 156*: 396-404.

Scholten D, Trebicka J, Liedtke C and Weiskirchen R (2015) The carbon tetrachloride model in mice. *Lab Anim 49*: 4-11.

Sha M, Gao Y, Deng C, Wan Y and Wang Y (2020) Therapeutic effects of AdipoRon on liver inflammation and fibrosis induced by CCl4 in mice. *International Immunopharmacology 79*: 106157-.

Sheffield LG and Berman N (1998) Microglial Expression of MHC Class II Increases in Normal Aging of Nonhuman Primates. *Neurobiology of Aging 19*: 47-55.

Shinotoh H, Snow BJ, Chu NS, Huang CC, Lu CS, Lee C, Takahashi H and Calne DB (1997) Presynaptic and postsynaptic striatal dopaminergic function in patients with manganese intoxication: A positron emission tomography study. *Neurology 48*: 1053-1056.

Shulman LM, Taback RL, Rabinstein AA and Weiner WJ (2002) Non-recognition of depression and other non-motor symptoms in Parkinson's disease. *Parkinsonism & Related Disorders 8*: 193-197.

Smeyne M, Goloubeva O and Smeyne RJ (2001) Strain-dependent susceptibility to MPTP and MPP(+)-induced parkinsonism is determined by glia. *Glia 34*: 73-80.

Spittau B (2017) Aging Microglia—Phenotypes, Functions and Implications for Age-Related Neurodegenerative Diseases. *Frontiers in Aging Neuroscience 9*: 194-.

Streit WJ and Sparks DL (1997) Activation of microglia in the brains of humans with heart disease and hypercholesterolemic rabbits. *Journal of Molecular Medicine 75*: 130.

Subramaniam SR and Federoff HJ (2017) Targeting Microglial Activation States as a Therapeutic Avenue in Parkinson's Disease. *Frontiers in Aging Neuroscience 9*: 176-.

Sugama S, Yang L, Cho BP, Degiorgio LA and Tong HJ (2003) Age-related microglial activation in 1-methyl-4-phenyl-1,2,3,6-tetrahydropyridine (MPTP)-induced dopaminergic neurodegeneration in

C57BL/6 mice. *Brain Research 964*: 288-294.

Sung YH, Kim SC, Hong HP, Park CY, Shin MS, Kim CJ, Seo JH, Kim DY, Kim DJ and Cho HJ (2012) Treadmill exercise ameliorates dopaminergic neuronal loss through suppressing microglial activation in Parkinson's disease mice. *Life Sciences 91*.

Sureka B, Bansal K, Patidar Y, Rajesh S, Mukund A and Arora A (2015) Neurologic Manifestations of Chronic Liver Disease and Liver Cirrhosis. *Current Problems in Diagnostic Radiology 44*: 449-461.

Surmeier DJ, Obeso JA and Halliday GM (2017) Selective neuronal vulnerability in Parkinson disease. *Nature Reviews Neuroscience 18*: 101-113.

Tan H, He Q, Li R, Lei F and Lei X (2016) Trillin Reduces Liver Chronic Inflammation and Fibrosis in Carbon Tetrachloride (CCl4) Induced Liver Injury in Mice. *Immunological investigations*: 1-12.

Tanaka S, Ishii A, Ohtaki H, Shioda S and Numazawa S (2013) Activation of microglia induces symptoms of Parkinson's disease in wild-type, but not in IL-1 knockout mice. *Journal of Neuroinflammation 10*: 143-143.

Tang Y and Le W (2016) Differential Roles of M1 and M2 Microglia in Neurodegenerative Diseases. *Molecular Neurobiology 53*: 1181-1194.

Tilg H (1992) Serum levels of cytokines in chronic liver diseases. *Gastroenterology 103*.

Toguchi M, Gonzalez D, Furukawa S and Inagaki S (2009) Involvement of Sema4D in the control of microglia activation. *Neurochemistry International 55*: 573-580.

Victoria L, Gurkarminder S and Sharon DM (2017) Recent advances in hepatic encephalopathy. *F1000research 6*: 1637.

Wang N, Liang Y, Devaraj S, Wang J, Lemon SM and Li K (2009) Toll-Like Receptor 3 Mediates Establishment of an Antiviral State against Hepatitis C Virus in Hepatoma Cells. *Journal of Virology 83*: 9824-9834.

Weissenborn K, Berding G and Köstler H (2000) Altered striatal dopamine D 2 receptor density and dopamine transport in a patient with hepatic encephalopathy. *Metabolic Brain Disease 15*: 173-178.

Wildon KE, Cai J and Lorraine I (2018) Regional microglia are transcriptionally distinct but similarly exacerbate neurodegeneration in a culture model of Parkinson's disease. *Journal of Neuroinflammation 15*: 139.

9. Publications

No

10. Declaration of contribution

The dissertation work was carried out at the Institute of Physiology, Department of Neurophysiology, of the Eberhard Karls Universität Tübingen under the supervision of Professor Dr. Olga Garaschuk and Dr. Bianca Brawek. The study was designed by Professor Dr. Olga Garaschuk. The brain tissue and the video recordings of the animal behaviour were obtained from our collaborators Dr. Yevsa Tetyana and Dr. Petriv Nataliia at Hannover Medical School (Medizinische Hochschule Hannover).

After training by laboratory members Professor Dr. Olga Garaschuk, Dr. Bianca Brawek, Dr. Yury Kovalchuk and technical assistant Elizabeta Zirdum, I labelled immunohistochemically, imaged and analyzed the stained tissue. The analyses of behaviour were carried by me and Dr. Bianca Brawek. Statistical analyses were carried out by myself under the supervision of Professor Dr. Olga Garaschuk and Dr. Bianca Brawek.

I confirm that I wrote the manuscript myself under the supervision of Professor Dr. Olga Garaschuk and Dr. Bianca Brawek and that any additional sources of information have been duly cited.

Date / signature of doctoral candidate

11. 08. 2021 Hui Wang

11. Acknowledgement

I want to express my deep gratitude to Professor Dr. Olga Garaschuk, Dr. Bianca Brawek and all the members of my doctoral project. I would like to thank the whole team of the Institute of Physiology, Department of Neurophysiology and Dr. Inka Montero and Professor Dr. Yevsa Tetyana and Dr. Petriv Nataliia at the Hannover Medical University. Without the invaluable support of these people, it would be not possible for me to accomplish this work.